S. S. S. SHABAN

OPTIMIZATION AND STANDARDIZATION OF FREE-FORM STEEL DOUBLE-LAYER GRIDS

THE GRADUATE SCHOOL OF NATURAL AND APPLIED SCIENCES
OF
ATILIM UNIVERSITY

SAMER S. S. SHABAN

A MASTER OF SCIENCE THESIS
IN
THE DEPARTMENT OF CIVIL ENGINEERING

JULY 2021

ATILIM UNIVERSITY

OPTIMIZATION AND STANDARDIZATION OF FREE-FORM STEEL DOUBLE-LAYER GRIDS

A THESIS SUBMITTED TO
THE GRADUATE SCHOOL OF NATURAL AND APPLIED SCIENCES
OF
ATILIM UNIVERSITY

BY

SAMER S. S. SHABAN

IN PARTIAL FULFILLMENT OF THE REQUIREMENTS
FOR
THE DEGREE OF MASTER OF SCIENCE
IN
THE DEPARTMENT OF CIVIL ENGINEERING

JULY 2021

Approval of the Graduate School of Natural and Applied Sciences, Atilim University.

_____

Prof. Dr. Ender Keskinkılıç
Director

I certify that this thesis satisfies all the requirements as a thesis for the degree of **Master of Science in Civil Engineering, Atilim University**.

_____

Asst. Prof. Dr. Saman Aminbakhsh
Acting Head of the Department

This is to certify that we have read the thesis "OPTIMIZATION AND STANDARDIZATION OF FREE-FORM STEEL DOUBLE-LAYER GRIDS" submitted by SAMER S. S. SHABAN and that in our opinion it is fully adequate, in scope and quality, as a thesis for the degree of Master of Science.

_____

Assoc. Prof. Dr. Saeid Kazemzadeh Azad
Supervisor

Examining Committee Members:

Prof. Dr. Eray Baran
Civil Eng. Dep., Middle East Technical University _____

Assoc. Prof. Dr. Saeid Kazemzadeh Azad
Civil Eng. Dep., Atilim University _____

Asst. Prof. Dr. Gökhan Tunç
Civil Eng. Dep., Atilim University _____

Date: *12.07.2021*

I hereby declare that all information in this document has been obtained and presented in accordance with academic rules and ethical conduct. I also declare that, as required by these rules and conduct, I have fully cited and referenced all material and results that are not original to this work.

Name, Last Name: Samer S. S. Shaban

Signature:

ABSTRACT

OPTIMIZATION AND STANDARDIZATION OF FREE-FORM STEEL DOUBLE-LAYER GRIDS

Shaban, Samer S. S.

M.S., Department of Civil Engineering

Supervisor: Assoc. Prof. Dr. Saeid Kazemzadeh Azad

July 2021, 52 pages

There has been a growing interest in the use of free-form structures with irregularly curved yet aesthetically pleasing configurations in the recent decades. Although design optimization of regular steel grids has been well addressed in the literature of structural optimization, still limited work has been devoted to optimum design of real-size free-form grid structures. On the one hand, a main obstacle when dealing with real-size free-form steel grids is the excessive computational effort associated with contemporary evolutionary optimization algorithms. On the other hand, it is generally perceived that the obtained final designs using conventional optimization algorithms may not necessarily be favored in practice if certain provisions are not stipulated by the algorithm to preclude an abundance of distinct steel section sizes in the final design. Hence, instead of offering a single optimum or near optimum design, it would be more desirable to provide the designer or decision maker with a Pareto front set of non-dominated design alternatives taking into account both the minimum weight as well as the assortment of available steel section sizes in the final design. Accordingly, in this paper, a computationally efficient multi-stage guided stochastic search algorithm is proposed for optimization and standardization of real-size free-form steel double-layer grids. A gradual design-oriented section elimination approach is followed where in the first optimization stage, a complete set of commercially available steel sections is introduced to the algorithm and in the succeeding stages, the size of section

list is reduced by eliminating the redundant sizes. Two variants of the algorithm are employed to demonstrate the usefulness of the proposed technique in challenging test examples of free-form steel double-layer grids, and the obtained Pareto fronts are plotted to illustrate the trade-off between minimum weight and assortment of steel section sizes in the final design.

Keywords: Design optimization, free-form structures, standardization, multi-stage guided stochastic search, steel double-layer grids, Pareto front.

ÖZ

SERBEST BİÇİMLİ ÇELIK ÇİFT KATMANLI UZAY KAFESLERİN OPTİMİZASYONU VE STANDARDİZASYONU

Shaban, Samer S. S.
Yüksek Lisans, İnşaat Mühendisliği Bölümü
Tez Yöneticisi: Doç. Dr. Saeid Kazemzadeh Azad

Temmuz 2021, 52 sayfa

Son yıllarda düzensiz eğrili ancak estetik açıdan hoş görünen konfigürasyonlara sahip serbest biçimli yapıların kullanımına artan bir ilgi olmuştur. Normal çelik uzay kafeslerin tasarım optimizasyonu, yapısal optimizasyon literatüründe detaylı bir şekilde ele alınsa da, gerçek boyutlu serbest biçimli uzay kafes yapıların optimum tasarımında yapılan çalışmalar hala sınırlı düzeyde kalmıştır. Bir yandan, gerçek boyutlu serbest biçimli çelik kafeslerin optimizasyonunun önündeki ana engel, güncel evrimsel optimizasyon algoritmalarıyla ortaya çıkan aşırı hesaplama yüküdür. Öte yandan, algoritma tarafından nihai tasarımda farklı çelik kesit boyutlarının sayıca fazlalığını önlemek için gerekli kısıtlamalar uygulanmamışsa, geleneksel optimizasyon algoritmaları kullanılarak elde edilen nihai tasarımların uygulamada tercih edilmemesi muhtemeldir. Bu nedenle, tek bir optimum veya optimuma yakın tasarım sunmak yerine, tasarımcıya veya karar vericiye, hem minimum ağırlığı hem de mevcut ürün çeşitliliğini hesaba katan ve etkin tasarım alternatifleri setinden oluşan bir Pareto eğrisi sunmak daha arzu edilir olacaktır. Buna göre, bu çalışmada, gerçek boyutlu serbest biçimli çelik çift katmanlı uzay kafeslerin optimizasyonu ve standardizasyonu için hesaplama açısından verimli çok aşamalı rehberli stokastik arama algoritması önerilmiştir. İlk optimizasyon aşamasında, algoritmaya ticari olarak mevcut çelik profillerin eksiksiz bir setinin sunulduğu ve sonraki aşamalarda, kullanılmayan veya daha az kullanılan kesitleri eleyerek kesit listesinin kademeli

olarak küçültüldüğü, bir tasarım odaklı kesit eleme yaklaşımı izlenmiştir. Serbest biçimli çelik çift katmanlı uzay kafeslerin sıra dışı kolay olmayan test örnekleri üzerinde önerilen tekniğin kullanışlılığını göstermek için algoritmanın iki farklı versiyonu kullanılmış ve elde edilen Pareto eğrisi, minimum ağırlık ve çelik kesit çeşitleri arasındaki dengeyi göstermek için çizilmiştir.

Anahtar Kelimeler: Tasarım optimizasyonu, serbest biçimli yapılar, standardizasyon, aşamalı rehberli stokastik arama, çelik çift katmanlı uzay kafesler, Pareto eğrisi.

To My Family

ACKNOWLEDGMENTS

I would like to express my sincere gratitude to my supervisor Assoc. Prof. Dr. Saeid Kazemzadeh Azad for his guidance and continuous encouragement that motivated me at all levels of the present thesis study. It was a great opportunity for me to work under his enlightening supervision.

In particular, I am thankful to my family for their encouragement and support throughout my thesis work.

I shall also thank to Asst. Prof. Dr. Saman Aminbakhsh for his guidance related to the use of Formian-2 software.

TABLE OF CONTENTS

LIST OF TABLES

TABLES

LIST OF FIGURES

FIGURES

CHAPTER 1

INTRODUCTION

1.1 Optimization of Free-Form Space Structures

Free-form space structures possessing irregularly curved architectural configurations have received considerable attention in building industry during the past few decades [1]. The increasing popularity of free-form space structures with innovative and aesthetically pleasing shapes can be attributed to the recent advancements in computer-aided design and construction technologies. Nevertheless, due to the existence of complex geometrical patterns as well as numerous structural members, modeling, and design optimization of real-size free-form space structures entail overcoming particular obstacles, some of which are outlined in the following.

A common challenge when dealing with free-form space structures is to generate the associated complex configurations in a convenient manner. One way of circumventing this problem is to produce the corresponding complex geometries via the concepts of formex algebra, using the programming language Formian [2-5]. Developing structural configurations using formex algebra for compound and free-form space structures with different geometrical characteristics has been well addressed in Moghimi [6]. The study provides formex formulations as well as useful guidelines to create complex, yet innovative geometries for various types of compound and free-form structures. Later, Nooshin and Moghimi [7] illustrated the usefulness of two formex concepts, namely pellevation and novation, in generating structural surfaces with free-form geometries. Recently, in a different approach, Gao et al. [8] proposed a grid generation method on free-form surfaces for lattice structures using the guide line method with surface flattening. Further details associated with alternative grid generation techniques on free-form surfaces can be found in Refs. [9-11].

Computer-aided design optimization has long been recognized as an efficient approach to minimize the weight or cost of steel skeletal structures for which a plethora of sophisticated algorithms have been developed so far. In contrast to traditional structural optimization techniques, which were generally proposed on the basis of mathematical programming [12] and optimality criteria [13, 14] concepts, contemporary optimization algorithms devised for optimal design of steel skeletal structures mostly belong to the class of metaheuristics [15, 16]. The popularity of metaheuristic structural optimization algorithms can be attributed to their derivative-free formulations, global search features, and capability of handling both discrete and continuous design variables. In spite of considerable research work conducted on metaheuristic optimization of steel skeletal structures [17-25], still research on optimum design of free-form structural systems using contemporary optimization algorithms is very limited. In a recent study, Kociecki and Adeli [26] investigated the design optimization of free-form steel space-frame roof structures with complex geometries using a modified genetic algorithm. The efficiency of the proposed methodology was demonstrated by means of two real-life design optimization instances of free-form steel space-frame roof structures considering architectural requirements.

On the other hand, to examine the performance of the developed optimization algorithms against challenging test examples of steel skeletal structures, it is common in the recent literature of structural optimization, to seek the optimal solution for such structures using relatively large sets of commercially available steel profiles. Although using a large set of commercial profiles increases the complexity of the investigated structural optimization problems and helps to better verify the performance of proposed techniques in more challenging test cases, the obtained final designs may not be necessarily favored in practice if certain provisions are not stipulated by the optimization algorithm to preclude an abundance of distinct steel profiles in the final design. In engineering practice, the privilege of structures composed of smaller number of steel profile types can be attributed to the cost efficiency of bulk purchasing and ease of fabrication and construction [27, 28]. In general, optimum structural standardization [29] deals with the optimal assortment of structural member sizes considering the economy of bulk purchasing or more comprehensively the overall

economy of construction. Reitman and Hall [29] formulated the structural optimization problem as an assortment problem that involves manufacturing costs and economy of scale. The study presented simultaneous design optimization and standardization of structural members through optimization of the structural properties of members as well as the assortment of sizes.

Templeman [27] pointed out the practical disadvantages of truss structures composed of numerous steel profile sizes due to the need to purchase, store, and fabricate small quantities of various commercial steel profiles that are slightly different in size. Accordingly, constraining the number of distinct sections in the final design to a small subset of a given list of available profiles has been addressed in the literature as cardinality constraints [28, 30] for which specific algorithms capable of handling these constraints have been devised. On the other hand, cardinality constraints and member grouping can be considered as two tightly related issues that enforcing the former could help the designer handle the latter and vice versa [28]. Although grouping the structural members can limit the maximum number of distinct sections in the final design to the number of member groups, often a suitable member grouping scheme in not known prior to solving the structural optimization problem. An initial intuitive member grouping based on experience and skills of the structural engineer becomes even more arduous in the case of geometrically irregular structures such as free-form steel double-layer grids where detecting similarities between members in terms of structural behavior is not trivial. One way to circumvent the difficulty of intuitive member grouping is to employ optimization algorithms capable of automatic member grouping in the course of optimization. In [28], a genetic algorithm encoding method was proposed that facilitates automatic member grouping by imposing the cardinality constraints. In their approach, a specific number (determined by cardinality constraint) of design variables in a candidate solution (chromosome) was devoted to identifying the best subset of available sections to be used for structural members. The efficiency of the proposed encoding method was demonstrated through minimum weight design optimization of benchmark instances, namely a 10-bar truss, a 47-bar truss, a 160-bar truss, and a 200-bar truss structure considering different cardinality constraints and member grouping schemes.

Angelo et al. [30] employed ant colony optimization algorithm for multi-objective optimization of truss structures under different cardinality constraint levels. Therein, minimization of two conflicting objectives, namely weight and maximum displacement of truss structures was carried out for each cardinality constraint level and the obtained Pareto fronts were illustrated. The study indicated the usefulness of the proposed metaheuristic-based methodology for multi-objective structural optimization using standard examples of truss structures with up to 59 independent discrete sizing variables. In a pioneering study, Galante [31] considered structural weight and number of cross-section types as two attributes for minimization in multi-objective optimization of truss structures using genetic algorithms. The multi-objective optimization problem was converted into single-objective optimization by combining the aforementioned two objectives using the traditional weighted sum method [32]. Shea et al. [33] developed a shape annealing method capable of dynamic grouping of members based on cross-sectional area for topology optimization of truss structures. The authors investigated the trade-off between the number of member groups, that affects material purchase and fabrication costs, and the optimum mass of truss structures through introducing a weighted group penalty function to the objective function.

Carvalho et al. [34] performed sizing and geometry optimization of truss structures with multiple frequency constraints and automatic member grouping. A metaheuristic algorithm based on particle swarm optimization was employed in conjunction with an adaptive penalty method [35] for constraint handling. The authors adopted cardinality constraints to seek the best member grouping for the structural members and demonstrated the efficiency of the employed metaheuristic-based approach using six test examples of planar and space truss structures. Moreover, the study presented the trade-off between the optimized weights versus the number of distinct cross-sectional areas in the final designs considering different cardinality constraint levels. In a recent study, Carvalho et al. [36] investigated simultaneous sizing, shape, and layout optimization of dome structures with automatic member grouping. The authors used differential evolution optimization algorithm [37], with a specific encoding for handling cardinality constraints, and presented trade-off curves depicting the

optimized design weights versus the number of different cross-sectional areas utilized in the final designs of truss dome structures.

A benchmark for assessing the optimality of different member grouping schemes could be obtained by solving the sizing optimization problem without member grouping where an independent design variable is assigned to each structural member. It is obvious that for large-scale structural systems this approach will produce challenging design optimization problems including numerous solution variables. Although in the case of structures with regular geometrical shapes it could be possible to reduce the number of design variables by initial variable linking, as already noted, this would be cumbersome for geometrically irregular structures such as free-form steel double-layer grids. Consequently, for these structures the problem of sizing optimization without member grouping would involve numerous discrete variables for which suitable algorithms should be adopted.

Despite previous successful applications of metaheuristics to investigate the trade-off between the number of different section types used in the final design and the minimum weight of truss structures with small or medium number of design variables, it is generally perceived that in the case of large-scale structural systems with thousands of discrete variables, obtaining optimum or near optimum solutions by means of metaheuristics is not possible in a timely manner. Essentially, the computational inefficiency of metaheuristics in high-dimensional structural optimization problems can be attributed to the myriad structural response computations required for convergence of these algorithms in higher dimensions. Indeed, the process of searching for an optimum design becomes much more cumbersome by increasing the problem dimensions referred to as the curse of dimensionality [38, 39]. To circumvent this problem, use of computationally efficient design-driven techniques that utilize the domain knowledge to guide the search process has been advocated.

1.2 Scope and Outline of the Thesis

Guided stochastic search (GSS) [40] is a recent design-oriented method devised for handling discrete sizing optimization problems with reasonable computational cost.

The algorithm uses a stochastic search technique where the sizing optimization process is guided by the principle of virtual work as well as the structural response computations of the candidate designs generated over the optimization iterations. Although the original version of the algorithm was developed for design optimization of steel trusses subject to a single displacement constraint under a single load case, thanks to the advantages of the integrated force method (IFM) [41], two alternative variants of the technique, i.e., GSS_A and GSS_B algorithms, have later been proposed to deal with discrete sizing of truss structures with multiple displacement constraints and load cases [42]. Recently, the efficiency of the foregoing two variants of the GSS in handling high-dimensional sizing optimization instances of steel truss structures has been examined in Ref. [43]. It was shown that the above-mentioned GSS based approaches are capable of handling high-dimensional examples of large-scale steel truss structures with thousands of discrete design variables for which contemporary metaheuristic techniques often fall short of providing promising solutions in a timely manner.

Owing to the promising performance of the GSS based techniques in the previous studies, in the present thesis, a multi-stage guided stochastic search (MS-GSS) method is proposed to investigate the trade-off between the number of distinct steel section types used in the final design and the minimum weight of free-form steel double-layer grids with numerous discrete variables. The algorithm works on the basis of a gradual design-oriented reduction of the set of available steel profiles and repeating the optimization process using the newly updated smaller subset of the complete list of sections. Accordingly, in the MS-GSS, a multi-stage run of the algorithm entails running multiple stages of design optimization where at each stage the algorithm is allowed to use an updated subset of the complete set of available steel sections. To this end, the best feasible solution obtained from the preceding optimization stage is used to identify the redundant sections. In the present study, redundant sections are unused steel sections or sections with minimum contribution to the total weight of the best feasible design achieved at the end of each optimization stage. These sections are eliminated from the section list due to their minor contribution to the total design weight and the resulting reduced section list is utilized in the succeeding optimization stage. Based on the above-mentioned GSS_A and GSS_B heuristics, two variants of the

MS-GSS are developed herein to study the trade-off between the number of different steel profiles utilized in the final design and the minimum weight of free-form steel double-layer grids. The usefulness of the proposed MS-GSS based techniques is demonstrated through challenging test examples of free-form steel double-layer grids, namely a 1900-member free-form grid, a 1952-member free-form grid, a 2080-member free-form grid, and a 2240-member free-form grid, and the obtained Pareto fronts illustrating the foregoing trade-off are elaborated.

The organization of this thesis is as follows. In Chapter 2, optimization problem formulation for minimum weight design of steel grids with discrete sizing variables is described. Chapter 3 presents the formulations for calculating the member sensitivity indices based on the principle of virtual work. In Chapter 4, the main steps of the proposed MS-GSS algorithm as well as its two variants are outlined. Chapter 5 presents the numerical experiments performed via the proposed MS-GSS algorithm for optimization and standardization of four challenging examples of free-form steel double-layer grids. The last chapter outlines the concluding remarks.

CHAPTER 2

STATEMENT OF THE SIZING OPTIMIZATION PROBLEM

2.1 Design Optimization Formulation per AISC-LRFD

As will be further described in the subsequent chapters, the approach followed in the present study to produce Pareto fronts via the proposed MS-GSS based techniques, can be categorized as a specific case of conventional ε-constraint method [44] where at each optimization stage a bi-objective optimization problem is transformed into a single-objective weight minimization instance. This section presents the corresponding single-objective optimization problem formulation for pin-jointed free-form steel double-layer grids with discrete sizing variables according to AISC-LRFD [45] specification. Here, the aim of design optimization is to find a vector of integer values **I** (Eq. 1) denoting the sequence numbers of steel sections in a set of commercially available profiles,

$$\mathbf{I}^T = \left[I_1, I_2, ..., I_{N_m}\right] \tag{1}$$

to produce a vector of cross-sectional areas **A** (Eq. 2) for N_m members of the steel grid,

$$\mathbf{A}^T = [A_1, A_2, ..., A_{N_m}] \tag{2}$$

such that **A** minimizes the associated weight objective function expressed as:

$$W = \sum_{i=1}^{N_m} \rho_i L_i A_i \tag{3}$$

where W is the net weight of the steel grid, ρ_i, L_i, A_i are unit weight, length, and cross-sectional area of the *i-th* structural element, respectively. The weight minimization problem mentioned above shall be tackled subject to the following strength and

displacement constraints. In accordance with AISC-LRFD [45], the following strength constraint shall be satisfied for each steel grid member *i*,

$$\left[\frac{P_u}{\phi P_n}\right]_i - 1 \le 0 \tag{4}$$

where P_u and P_n are the required and nominal axial (tensile or compressive) strengths of the considered *i-th* grid member, respectively. In the above equation, ϕ is the resistance factor for axial strength, taken as 0.85 for compression and 0.9 for tension. As per AISC-LRFD [45], the nominal tensile strength of a member, based on yielding in the gross cross section, is computed using the following relation:

$$P_n = F_y A_g \tag{5}$$

where F_y is the member's specified yield stress and A_g is the gross cross section of the member. Besides, the nominal compressive strength of members with compact and/or non-compact elements, for the limit state of flexural buckling is determined as follows:

$$P_n = F_{cr} A_g \tag{6}$$

where F_{cr} is the critical stress based on flexural buckling of the member, calculated as:

for $\lambda_c = \frac{K l}{r \pi}\sqrt{\frac{F_y}{E}} \le 1.5$ $\qquad F_{cr} = (0.658^{\lambda_c^2})F_y$ (7)

for $\lambda_c = \frac{K l}{r \pi}\sqrt{\frac{F_y}{E}} > 1.5$ $\qquad F_{cr} = \left[\frac{0.877}{\lambda_c^2}\right]F_y$ (8)

In the above relations, l is the laterally unbraced length of the member, K is the effective length factor, r is the governing radius of gyration about the buckling axis and E is the modulus of elasticity. Meanwhile, in order to impose the displacement constraints, the following serviceability criterion shall be satisfied:

$$\frac{d_{j,k}}{(d_{j,k})_{all}} - 1 \leq 0 \tag{9}$$

where $j = 1, 2, \ldots, N_j$ is the joint number, N_j is the total number of joints, $d_{j,k}$, and $(d_{j,k})_{all}$, are the displacements computed in the *k-th* direction of the *j-th* joint and the associated allowable displacement, respectively.

CHAPTER 3

SENSITIVITY ANALYSIS

3.1 Sensitivity Index Calculation

The use of domain knowledge has been generally perceived as an efficient approach to enhance the computational efficiency of the contemporary design optimization algorithms. In the context of sizing optimization of free-form steel double-layer grids, while load-capacity ratios determined through Eq. (4) can be readily used to handle the strength constraints, handling the displacement constraints entails calculating the contribution of each member to the total displacement in the direction of interest, namely the so-called displacement participation factor (DPF) [46]. In order to compute the DPF of a grid element in the *k-th* direction of the *j-th* joint, in addition to a regular structural analysis carried out under the applied real loads, the steel grid structure should also be analyzed under a virtual unit load applied at the same joint and in the same direction. The corresponding DPF of the *i-th* element in the *k-th* direction, denoted by $DPF_{i,k}$, can subsequently be calculated using the following equation,

$$DPF_{i,k} = \frac{P_i^r P_i^u}{E_i A_i} L_i \tag{10}$$

where P_i^r and P_i^u are the internal axial forces in the *i-th* element under the real and unit loads, respectively. In the foregoing equation, E_i, A_i, and L_i denote the modulus of elasticity, cross-sectional area, and length of the *i-th* member, respectively. It is obvious that the total displacement of the steel grid in the *k-th* direction, $\delta_{Total,k}$, can readily be computed by summing the corresponding DPF values as:

$$\delta_{Total,k} = \sum_{i=1}^{N_m} DPF_{i,k} \tag{11}$$

Although some studies advocate the direct formulation of the DPF for drift control of buildings [47], it could be more fruitful to employ the concept of sensitivity index (SI) [48] for design optimization since it is a superior indicator to determine the efficiency of the structural elements in satisfying the displacement criteria by taking into account the volume of elements as follows:

$$SI_{i,k} = \frac{DPF_{i,k}}{V_i} \tag{12}$$

where $SI_{i,k}$ and V_i are the sensitivity index in the *k-th* direction, and volume of the *i-th* element, respectively. The calculated SI values will subsequently be used to guide the optimization process as described in the next chapter.

CHAPTER 4

DESIGN-DRIVEN OPTIMIZATION TECHNIQUE

4.1 Multi-Stage Guided Stochastic Search

Guided stochastic search (GSS) optimization algorithm is a recently developed design-driven heuristic method for computationally efficient discrete sizing optimization [40, 42]. The algorithm works based on a stochastic search approach where the optimization process is guided by the principle of virtual work as well as the structural responses computed during the iterations of the algorithm. Considering the promising performance of the GSS based approaches, a multi-stage guided stochastic search (MS-GSS) method is developed to study the trade-off between the number of distinct steel section sizes used in the final design and the optimal weight of free-form steel double-layer grids. It is aimed to visualize the foregoing trade-off through Pareto front sets that can be used for subsequent standardization of the investigated structures. Pareto front tracing for free-form steel double-layer grids via MS-GSS algorithm consists of the following multi-stage process.

Step 1. Run initialization: A multi-stage run of the algorithm involves running multiple stages of design optimization where at each stage the algorithm is allowed to use a newly updated list of available steel sections. In other words, a multi-stage run is executed as an outer loop of optimization code while the inner loops deal with different dependent stages of design optimization. A multi-stage run starts by setting the prespecified algorithm parameters to their initial values.

Step 2. Stage initialization: The corresponding list of available steel sections to be used for sizing the structural members is uploaded. In the first stage, a complete set of steel sections is introduced to the algorithm whereas in the succeeding stages the size of section list is reduced by eliminating the redundant sections. The associated elimination process is described in Step 9. At each stage of MS-GSS, discrete sizing

optimization starts with a randomly generated candidate design. It is worthwhile to note that in the present algorithm, design variables generated beyond the predetermined ranges are set to their lower or upper limit values.

Step 3. Evaluation under real loading: The newly produced candidate solution is analyzed with application of real loads, where structural response computations are accomplished using the set of steel sections assigned to the design variables. Once element forces and nodal displacements are determined, feasibility of the free-form steel double-layer grid is examined using Eqs. (4-9) and possible strength and displacement constraint violations are identified accordingly. This step evaluates the feasibility of the produced candidate solution at each iteration of the current optimization stage. It is noteworthy to point out that each stage of MS-GSS algorithm consists of a definite number of optimization iterations after which the best feasible solution of the stage is saved.

Step 4. Evaluation under virtual loading: Beside the aforementioned evaluation of the candidate solution under the acting real loads on the double-layer grid, typically an additional evaluation is required at this step to determine the structural response under the virtual loading in order to calculate the SI values by Eq. (12). Nevertheless, it is demonstrated in Ref. [42] that using the IFM [41], it is possible to obtain the virtual internal forces in structural members developed under an applied virtual load based on the structural analysis already performed in Step 3. Hence, at each iteration of the optimization process, once the steel double-layer grid is analyzed under the applied real loads in the third step, the required virtual internal forces for SI calculations could be readily obtained without further structural response computations.

Step 5. Detection of critical members: The key to efficient guiding the search process is to identify the following two critical groups of double-layer grid elements for resizing. The first group is composed of those grid elements that will be increased in size to eliminate the strength and displacement constraint violations. In contrast, the second group of grid members consists of those elements that will be decreased in size in compliance with the weight minimization goal of the optimum design procedure. The selection of critical grid members for the foregoing two groups is accomplished as follows.

Step 5.1. Increase-group for constraint satisfaction: Double-layer grid members that will be increased in size in order to handle constraint violations, belong to the first group specified as increase-group (IG). This group of grid members which is devoted to constraint handling can further be divided into two subgroups as IG_s and IG_d based on whether an increase in member size is necessary due to strength criteria (IG_s) or displacement criteria (IG_d). Here, all the grid members that violate the strength constraints of the design optimization problem are directly assigned to the IG_s subgroup. These elements can readily be determined considering the load-capacity ratios (*LCR*s), Eq. (13), which exceed 1 for under-designed double-layer grid elements.

$$LCR = \left[\frac{P_u}{\phi P_n} \right] \tag{13}$$

Here, IG_d members are identified with respect to SI values determined by Eq. (12). Accordingly, grid members with higher SI values are specified as the most critical members for handling the displacement constraints. The number of IG_d members is determined by means of an adaptive ratio parameter R_d (see step 7) that stipulates the use of a specific percentage of the design variables for resizing.

Step 5.2. Decrease-group for weight reduction: Double-layer grid members that will be decreased in size to achieve a certain reduction in the design weight are assigned to the second group named as decrease-group (DG_w). To this end, first the most overdesigned steel grid members in terms of the strength criteria are identified based on LCR values. Next, they are further evaluated with respect to the corresponding SI values, and those members which have the least impact on the displacement criteria are selected as DG_w members. Hence, the DG_w group contains overdesigned grid members for which the size reduction is expected to have a minor effect on the displacement response of the structure in the direction of interest. Similar to the aforementioned IG_d members, the number of DG_w members is also determined using an adaptive ratio parameter R_w (see step 7) that facilitates the use of a specific percentage of the design variables in the resizing process.

Step 6. Stochastic member resizing: The MS-GSS works based on a simple stochastic approach for member resizing where the IG_s and IG_d members are

stochastically increased in size with respect to a prespecified maximum incremental step size. Here, the maximum incremental step size is set to $\sqrt{N_s}$ (rounded to the nearest integer) where N_s is the number of available steel sections to size the double-layer grid members. A random move towards larger steel sections is then carried out for each IG member by Eq. (14),

$$I_i^{new} = I_i^{pre} + Rand^{IG} \tag{14}$$

where I_i^{pre} is the value of a design variable in the previous iteration; I_i^{new} is the new value of the design variable, representing the sequence number of the new section selected for an IG member in the current iteration; and $Rand^{IG}$ is an integer random number chosen between 1 and the maximum incremental step size in accordance with a uniform distribution.

Meanwhile, the DG_w members are stochastically decreased in size according to a predetermined maximum decremental step size which is taken as maximum incremental step size minus two in the present study. For computations, maximum decremental step size is set to unity in case the corresponding value becomes less than one. A random move towards smaller sections is then carried out for each of the DG_w members as follows:

$$I_i^{new} = I_i^{pre} - Rand^{DG_w} \tag{15}$$

where $Rand^{DG_w}$ is an integer random number chosen between 1 and the maximum decremental step size based on a uniform distribution. The above-mentioned resizing scheme of the MS-GSS facilitates stochastic yet design oriented moves in the solution space to locate the optimum or a good near optimum solution.

Step 7. Updating the rate of member resizing: At each iteration, the number of steel grid members selected for resizing the grid structure is determined in this step. In this regard, an adaptive approach is employed with respect to the feasibility of the candidate design at each iteration based on the following rules. The first rule is that IG_s members, namely those violating the strength constraints, are all increased in size

considering the significance of the strength criteria for generating feasible designs. Secondly, as previously noted, not all but rather a certain percentage of double-layer grid members are chosen as DG_w and IG_d members for resizing with respect to the R_w, and R_d ratios. In this study, both the parameters are initially set to a minimum value of 0.1.

In order to facilitate an efficient weight reduction procedure, R_w ratio is increased by ΔR at each iteration if no constraint violation occurs in the generated candidate solution. It is obvious that, increasing the value of R_w will result in contribution of more grid members in weight reduction process. Nonetheless, in case of any constraint violation in the produced candidate solution, the value of R_w is set back to its initial value to accelerate the repair of the generated infeasible solution.

On the other hand, for IG_d members the initial value of $R_d = 0.1$ could be constant over the design optimization iterations. However, if no improvement is achieved in eliminating the displacement violations, the same adaptive strategy employed for R_w could be followed for R_d as well to further increase the number of double-layer grid elements contributing to satisfy the displacement criteria. It is worthwhile to note that in the present work, a maximum value of $R_{max} = 0.7$ is chosen for both R_w and R_d.

Step 8. Stage termination: The foregoing optimization process is iteratively performed, starting from the preceding candidate solution at each iteration, until a stopping criterion is met. The termination condition for each optimization stage of MS-GSS is taken as the maximum number of iterations which is set to 500 iterations in this study. Once the maximum number of iterations is reached, the corresponding optimization stage is terminated, and the obtained best feasible solution is saved.

Step 9. Updating the steel section list: Prior to starting the next optimization stage, it is necessary to update the list of available steel sections as follows. Here, the best feasible solution obtained from the preceding stage is used to identify the redundant sections. In this study, redundant sections are unused sections or sections with minimum contribution to the total design weight of the best feasible solution achieved at the end of each optimization stage. These sections are eliminated from the section list owing to their minor contribution to the total design weight and the resulting reduced section list is employed in the succeeding optimization stage. It is worth

mentioning that the rate of the aforementioned elimination of redundant sections over the optimization stages can be adjusted using a predefined reduction size (RS) parameter. This parameter indicates the minimum number of sections expected to be removed from the section list after each stage. It is obvious that the exact number of redundant sections can be greater than RS because of unused sections at an optimization stage. Thus, the number of redundant sections will be equal to sum of unused sections and reduction size parameter value. In the present study, the value of parameter RS is set to 1. It should also be noted that since the size of section list changes at every stage, the maximum incremental step size as well as maximum decremental step size parameters (see Step 6) are also updated at every stage, accordingly. Once the steel section list and the foregoing algorithm parameters are updated, the new optimization stage is initiated from Step 2.

Step 10. Run termination: A multi-stage run of the algorithm terminates if either: (*i*) the number of remaining steel sections in the section list reaches a minimum value that further reduction of the list is not possible with respect to RS parameter, or (*ii*) no feasible solution can be generated using the remaining list of steel sections. In some specific cases the latter could take place immediately after removing the least utilized steel section from the set of profiles. As a remedy, to preserve the feasibility of the design in such cases, instead of eliminating the least utilized steel section, alternatively, the second least utilized section can be eliminated to continue the search process. In case no feasible solution is achieved using the new set of profiles, the corresponding multi-stage run will be terminated. After termination of the multi-stage run, the number of steel sections used at each stage together with the associated best feasible design weights are saved for Pareto front tracing of free-form double-layer grids. It is apparent that due to the stochastic nature of the algorithm, multiple runs are necessary to better visualize the Pareto front. In order to further elaborate the optimization procedure using the MS-GSS, a general flowchart of the algorithm is shown in Figure 4.1.

As already noted, owing to the advantages of the IFM [41], two alternative variants of the GSS algorithm namely, GSS_A and GSS_B, have been developed to deal with discrete sizing optimization problems under multiple displacement constraints and load cases [42]. In the first approach, i.e., GSS_A the design optimization problem is treated akin

to a single displacement constraint problem by focusing only on the most critical displacement direction at each iteration, while in the second approach, i.e., GSS_B, multiple displacement constraints are considered on a cumulative basis to guide the design optimization process. It is demonstrated in Ref. [42] that the use of IFM [41] formulation relieves the additional computational burden of Step 4 at each iteration of the design optimization. In the present study, two variants of the MS-GSS, developed on the basis of the above-mentioned GSS_A and GSS_B heuristics, are referred to as MS-GSS_A and MS-GSS_B, respectively. The optimization results obtained via the proposed techniques based on the above-mentioned procedure, are subsequently post-processed to generate Pareto fronts as described in the next section.

4.2 Pareto Front Generation

The methodology used to generate Pareto fronts using the proposed MS-GSS based algorithms can be considered as a specific case of well-known ε-constraint method [44] where at each optimization stage a bi-objective optimization problem is transformed into a single-objective weight minimization case by limiting the maximum number of distinct steel sections in the final design to the size of the employed section list. By updating the size of the steel section list over different optimization stages, non-dominated solutions are sought for different subsets of the available steel profiles. In order to plot the Pareto fronts of free-form steel double-layer grids, first, the designs obtained over multiple runs of MS-GSS_A and MS-GSS_B algorithms are collected in a pool of solutions. Subsequently, non-dominated solutions amongst all the available designs in the pool of solutions are identified and associated Pareto fronts are plotted to visualize the trade-off between number of employed steel section sizes and corresponding design weights of the investigated free-form double-layer grids.

It is apparent that the best feasible solution for the case where only one of the profiles, from the complete set of available steel profiles, is to be assigned to all the structural members, can be readily obtained using a simple exhaustive enumeration. Here, prior to starting the optimization process, the corresponding trivial solution is identified and included in the above-mentioned pool of solutions.

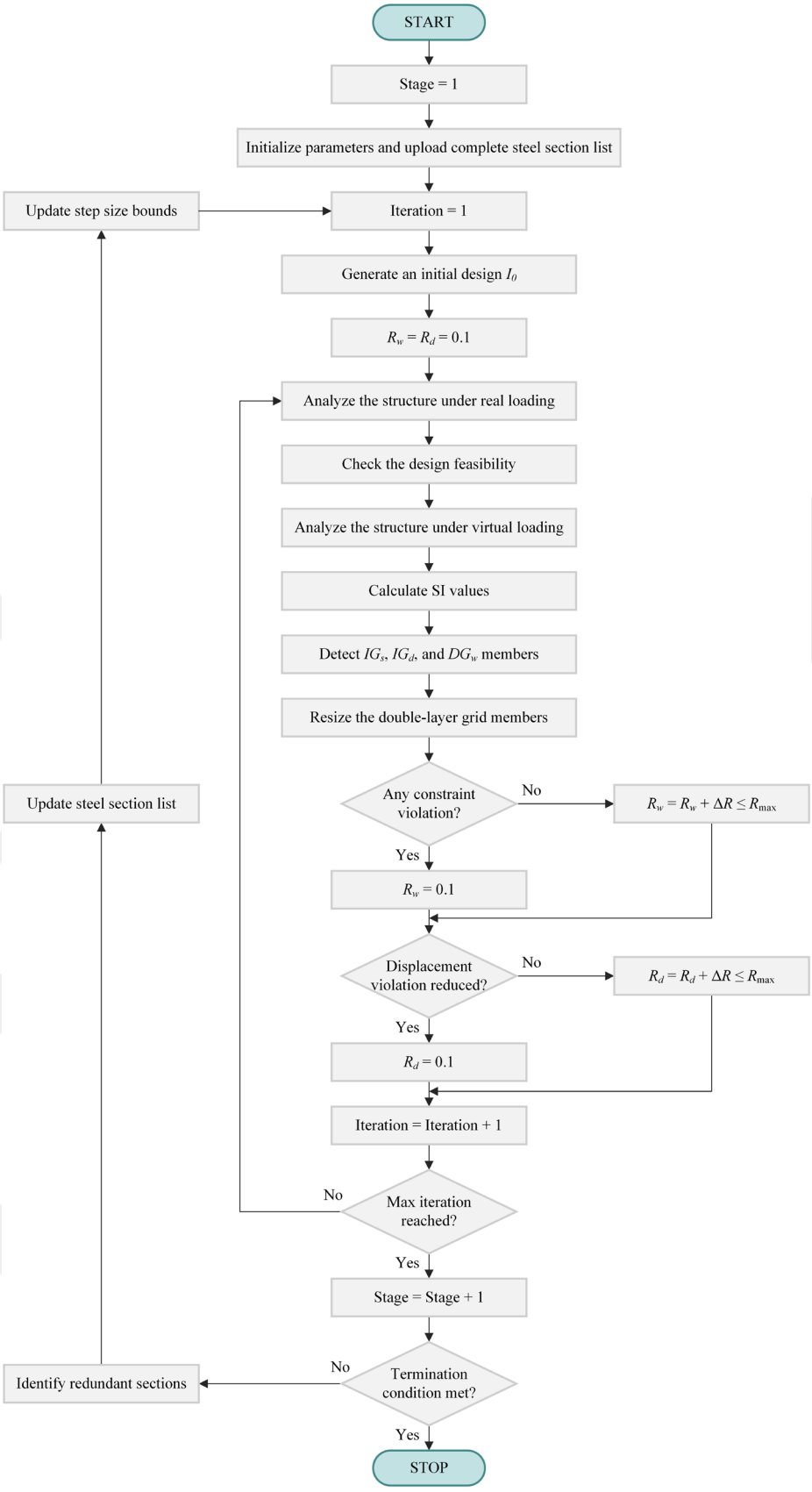

Figure 4.1 Flowchart of design optimization via MS-GSS algorithm

CHAPTER 5

NUMERICAL EXPERIMENTS

5.1 Design Optimization Examples

This section elaborates the numerical experiments performed via the proposed MS-GSS algorithm for optimization and standardization of four challenging instances of free-form steel double-layer grids, namely a 1900-member free-form grid, a 1952-member free-form grid, a 2080-member free-form grid, and a 2240-member free-form grid, and the obtained Pareto fronts illustrating the foregoing trade-off are elaborated. For each test example, the obtained Pareto front is plotted which shows the trade-off between design weight and number of distinct steel section sizes used in the final design. The provided Pareto fronts can subsequently be used by a decision-maker for optimum structural standardization with respect to the associated costs such as bulk purchasing or overall construction costs.

Considering the stochastic characteristics of the proposed MS-GSS_A and MS-GSS_B algorithms, each test example is tackled ten times using each algorithm, resulting in twenty multi-stage runs per example, and the results obtained are post-processed to identify the set of non-dominated solutions that form the presented Pareto fronts. For both the above-mentioned variants of MS-GSS algorithm, parameter ΔR is set to 0.1, and the maximum number of iterations per optimization stage is taken as 500. The set of 37 pipe sections [45] given in Table 5.1 is considered for sizing the investigated free-form double-layer grids. While the complete list of pipe sections is utilized in the first stage of each multi-stage run, as already stated, the size of section list changes at every stage due to the elimination of redundant sections. The material properties of steel are taken as follows: modulus of elasticity (E) = 200 GPa, yield stress (F_y) = 248.2 MPa, and unit weight of the steel (ρ) = 7.85 ton/m^3. In this study, the generic formex formulations outlined in [6] are considered to create the geometric configurations of

the investigated free-form steel double-layer grids. Besides, Formian-2 software [49] is used to extract the corresponding geometric data for structural analysis stage.

Table 5.1 Cross sectional properties of the available steel sections

Section no.	Designation	Area (cm^2)	Radius of gyration (cm)	Section no.	Designation	Area (cm^2)	Radius of gyration (cm)
1	PIPE1/2STD	1.6129	0.6624	20	PIPE3-1/2XS	23.7419	3.3181
2	PIPE1/2XS	2.0645	0.6350	21	PIPE2-1/2XXS	25.9999	2.1435
3	PIPE3/4STD	2.1484	0.8467	22	PIPE5STD	27.7419	4.7755
4	PIPE3/4XS	2.7935	0.8188	23	PIPE4XS	28.4516	3.7495
5	PIPE1STD	3.1871	1.0659	24	PIPE3XXS	35.2903	2.6580
6	PIPE1XS	4.1226	1.0345	25	PIPE6STD	35.9999	5.6999
7	PIPE1-1/4STD	4.3161	1.3713	26	PIPE5XS	39.4193	4.6752
8	PIPE1-1/2STD	5.1548	1.5821	27	PIPE4XXS	52.258	3.4909
9	PIPE1-1/4XS	5.6839	1.3312	28	PIPE6XS	54.1934	5.5773
10	PIPE1-1/2XS	6.9032	1.5354	29	PIPE8STD	54.1934	7.4621
11	PIPE2STD	6.9032	2.0039	30	PIPE5XXS	72.9031	4.3799
12	PIPE2XS	9.5484	1.9452	31	PIPE10STD	76.774	9.3427
13	PIPE2-1/2STD	10.9677	2.4097	32	PIPE8XS	82.5805	7.3094
14	PIPE3STD	14.3871	2.9559	33	PIPE12STD	94.1934	11.1035
15	PIPE2-1/2XS	14.5161	2.3464	34	PIPE6XXS	100.645	5.2363
16	PIPE2XXS	17.1613	1.7825	35	PIPE10XS	103.8708	9.2170
17	PIPE3-1/2STD	17.2903	3.3957	36	PIPE12XS	123.8707	11.0290
18	PIPE3XS	19.4838	2.8827	37	PIPE8XXS	137.4191	7.0049
19	PIPE4STD	20.4516	3.8360				

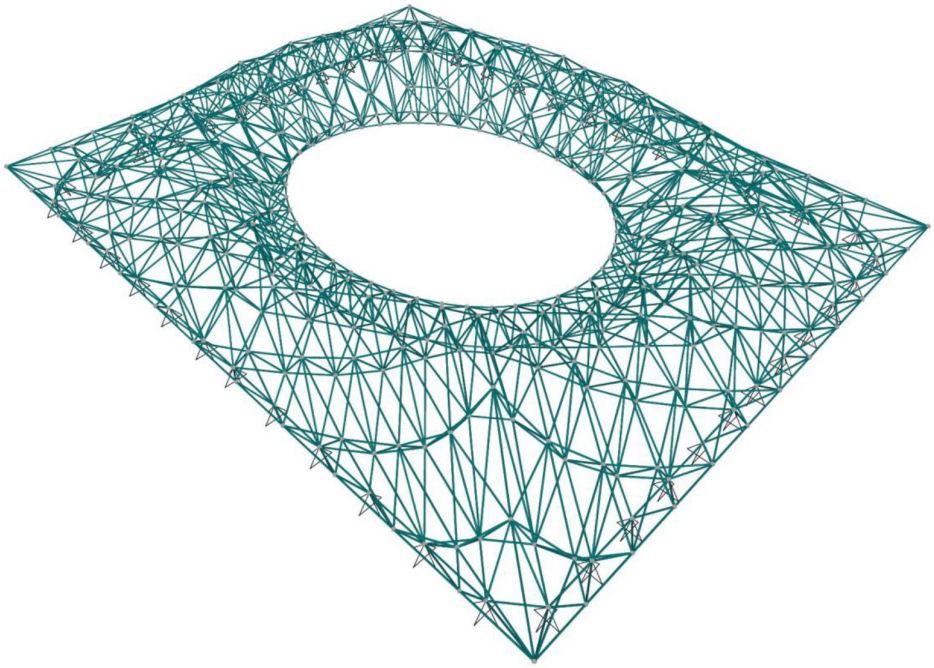

(a) perspective view

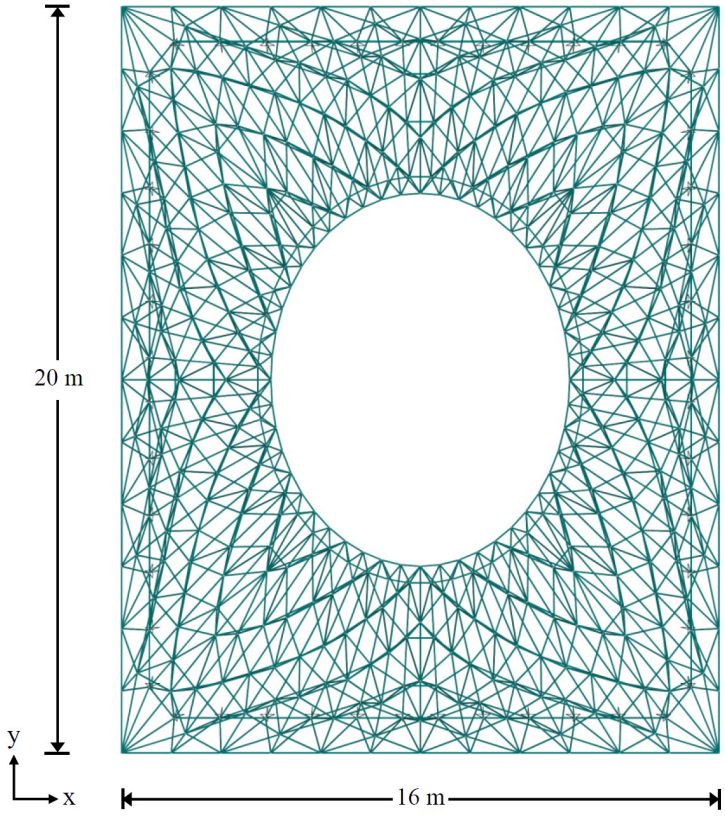

(b) plan view

Figure 5.1 1900-member free-form grid: (a) perspective view, and (b) plan view

5.1.1 Test Example 1: 1900-Member Free-Form Grid

The 1900-member free-form double-layer grid depicted in Figure 5.1 is considered as the first test example to study the assortment of steel section sizes in the final design. The grid comprises 1900 structural members and 480 joints. Here, sizing optimization problem of the free-form steel double-layer grid is tackled without member grouping which forms a challenging test case including 1900 distinct sizing design variables. The free-form double-layer grid is to be designed to resist the following three independent loading cases. Here, concentrated loads are applied at all the unsupported joints of the free-form double-layer grid in the following cases: (i) horizontal loads of 15 kN acting in the positive x-direction, (ii) horizontal loads of 15 kN acting in the positive y-direction, and (iii) vertical loads of 15 kN acting in the negative z-direction. The free-form grid shall be designed such that under the foregoing loading conditions the maximum displacement of all joints in the x, y, and z directions does not exceed 2.5 cm.

Multi-stage optimization of the 1900-member free-form double-layer grid is performed using the proposed MS-GSS$_A$ and MS-GSS$_B$ algorithms where in the first stage, the complete set of 37 steel sections presented in Table 5.1 is introduced to the algorithms and in the subsequent stages, size of the foregoing profile list is reduced by eliminating the redundant sections. Table 5.2 shows the contribution of different steel section sizes to the design weight of the best feasible solution, i.e., 21745.63 kg, obtained at the end of the first stage of the first multi-stage run of the MS-GSS$_A$. As can be seen from the table, steel section number 16, namely PIPE2XXS, is the most utilized profile in the best feasible design that forms 5.78% of the total weight of the final design. In contrast, steel section number 2, i.e., PIPE1/2XS is the least utilized steel section with only 0.32% contribution to the total design weight. Hence, at the end of the first stage, PIPE1/2XS is identified as one of the redundant section sizes which will be eliminated from the list of available profiles prior to starting the second stage. Table 5.3 presents the utilized sections in the final design of each stage for the first multi-stage run of the MS-GSS$_A$ algorithm. Here, for the sake of brevity the results are illustrated only for the initial fifteen stages of the algorithm. The remaining stages are accomplished in a similar way where at each optimization stage the profile list is

updated via detecting the redundant sections. Bearing in mind that redundant sections can be either unused sections or sections with minimum contribution to the total weight of the best feasible design, it can be deduced from Tables 5.2 and 5.3 that the above-mentioned PIPE1/2XS is not the only redundant section identified at the end of the first optimization stage. It is apparent from Table 5.3 that although 37 pipe sections are introduced to the algorithm at the beginning of the first optimization stage, the final design does not contain PIPE6XXS, PIPE10XS, PIPE12XS, and PIPE8XXS sections. Consequently, for the investigated 1900-member free-form double-layer grid totally five distinct sections, namely PIPE1/2XS, PIPE6XXS, PIPE10XS, PIPE12XS, and PIPE8XXS, with associated section numbers 2, 34, 35, 36, and 37, are identified as redundant sections at the end of the first stage. These sections are then eliminated from the complete list of 37 pipe sections resulting in a smaller subset of profiles including 32 section sizes employed to start the next optimization stage.

Figure 5.2 shows the convergence histories of optimization for the 1900-member free-form grid, in the first stage of the first multi-stage run, using the MS-GSS_A and MS-GSS_B algorithms. Although the maximum number of iterations per optimization stage is taken as 500, the best feasible solution is often located earlier. As shown in the figure, MS-GSS_A and MS-GSS_B locate the best feasible solution in the above-mentioned first optimization stage after 277 and 184 iterations, respectively. It is important to note that, since only one structural analysis is carried out per iteration, these values reflect the number of structural analyses as well. Tables 5.4 and 5.5 present the number of structural analyses corresponding to the iteration number at which the best feasible design is obtained for the 1900-member free-form grid. The presented results belong to the initial fifteen stages of the first multi-stage run using the proposed MS-GSS_A and MS-GSS_B algorithms. As already noted, once multi-stage runs are accomplished ten times for each algorithm, the obtained best feasible designs over multiple runs of the algorithms are collected in a pool of designs. Subsequently, non-dominated solutions are specified, and corresponding Pareto fronts are plotted to visualize the trade-off between number of utilized section sizes and weights of the free-form double-layer grids. Figure 5.3 presents the Pareto front corresponding to the 1900-member grid test example and visualizes the trade-off between weight and number of steel section sizes. The provided Pareto fronts can subsequently be

employed by a decision-maker for optimum structural standardization with respect to the associated costs such as bulk purchasing or overall construction costs.

Table 5.2 Contribution of steel section sizes to the design weight of 1900-member grid using MS-GSS$_A$

Section no.	Designation	Area (cm^2)	Total length (m)	Total weight (kg)	% of grid weight
16	PIPE2XXS	17.1613	93.29	1256.72	5.78
24	PIPE3XXS	35.2903	44.39	1229.68	5.65
26	PIPE5XS	39.4193	39.11	1210.31	5.57
25	PIPE6STD	35.9999	37.90	1070.97	4.92
27	PIPE4XXS	52.2580	24.53	1006.21	4.63
10	PIPE1-1/2XS	6.9032	176.26	955.16	4.39
28	PIPE6XS	54.1934	22.40	953.12	4.38
29	PIPE8STD	54.1934	19.75	840.36	3.86
23	PIPE4XS	28.4516	37.31	833.19	3.83
12	PIPE2XS	9.5484	110.01	824.58	3.79
21	PIPE2-1/2XXS	25.9999	39.93	814.93	3.75
13	PIPE2-1/2STD	10.9677	83.86	722.02	3.32
11	PIPE2STD	6.9032	127.74	692.20	3.18
6	PIPE1XS	4.1226	203.15	657.44	3.02
14	PIPE3STD	14.3871	57.96	654.56	3.01
9	PIPE1-1/4XS	5.6839	141.34	630.66	2.90
15	PIPE2-1/2XS	14.5161	52.44	597.53	2.75
30	PIPE5XXS	72.9031	10.32	590.86	2.72
17	PIPE3-1/2STD	17.2903	42.33	574.54	2.64
19	PIPE4STD	20.4516	34.77	558.27	2.57
20	PIPE3-1/2XS	23.7419	29.79	555.24	2.55
31	PIPE10STD	76.7740	9.15	551.15	2.53
22	PIPE5STD	27.7419	24.15	525.91	2.42
5	PIPE1STD	3.1871	205.77	514.82	2.37
18	PIPE3XS	19.4838	33.23	508.26	2.34
32	PIPE8XS	82.5805	7.34	475.73	2.19
7	PIPE1-1/4STD	4.3161	133.59	452.62	2.08
8	PIPE1-1/2STD	5.1548	103.17	417.49	1.92
1	PIPE1/2STD	1.6129	315.00	398.83	1.83
4	PIPE3/4XS	2.7935	157.32	345.00	1.59
3	PIPE3/4STD	2.1484	94.82	159.92	0.74
33	PIPE12STD	94.1934	1.32	97.72	0.45
2	PIPE1/2XS	2.0645	42.95	69.61	0.32
Total				21745.63	100

Table 5.3 Multi-stage elimination of redundant sections for 1900-member grid via MS-GSS$_A$

Designation		MS-GSS$_A$ optimization stage no.														
		1	2	3	4	5	6	7	8	9	10	11	12	13	14	15
1	PIPE1/2STD	1	1	1	1	1	1	1	1	[]*	[]	[]	[]	[]	[]	[]
2	PIPE1/2XS	2	[]	[]	[]	[]	[]	[]	[]	[]	[]	[]	[]	[]	[]	[]
3	PIPE3/4STD	3	3	[]	[]	[]	[]	[]	[]	[]	[]	[]	[]	[]	[]	[]
4	PIPE3/4XS	4	4	4	4	4	4	4	4	4	4	4	4	4	4	4
5	PIPE1STD	5	5	5	5	5	5	5	5	5	[]	[]	[]	[]	[]	[]
6	PIPE1XS	6	6	6	6	6	6	6	6	6	6	6	6	6	6	6
7	PIPE1-1/4STD	7	7	7	7	7	7	7	7	7	7	7	7	7	7	[]
8	PIPE1-1/2STD	8	8	8	8	8	[]	[]	[]	[]	[]	[]	[]	[]	[]	[]
9	PIPE1-1/4XS	9	9	9	9	9	9	9	9	9	9	9	9	9	9	9
10	PIPE1-1/2XS	10	10	10	10	10	10	10	10	10	10	10	10	10	10	10
11	PIPE2STD	11	11	11	11	11	11	11	11	11	11	11	11	11	11	11
12	PIPE2XS	12	12	12	12	12	12	12	12	12	12	12	12	12	12	12
13	PIPE2-1/2STD	13	13	13	13	13	13	13	13	13	13	13	13	13	13	13
14	PIPE3STD	14	14	14	14	14	14	14	14	14	14	14	14	14	[]	[]
15	PIPE2-1/2XS	15	15	15	15	15	15	15	15	15	15	15	15	15	15	15
16	PIPE2XXS	16	16	16	16	16	16	16	16	16	16	16	16	16	16	16
17	PIPE3-1/2STD	17	17	17	17	[]	[]	[]	[]	[]	[]	[]	[]	[]	[]	[]
18	PIPE3XS	18	18	18	18	18	18	18	18	18	18	[]	[]	[]	[]	[]
19	PIPE4STD	19	19	19	19	19	19	19	19	19	19	19	19	19	19	19
20	PIPE3-1/2XS	20	20	20	20	20	20	20	20	20	20	20	20	20	20	20
21	PIPE2-1/2XXS	21	21	21	21	21	21	21	21	21	21	21	21	21	21	21
22	PIPE5STD	22	22	22	22	22	22	22	22	22	22	22	22	[]	[]	[]
23	PIPE4XS	23	23	23	23	23	23	23	23	23	23	23	23	23	23	23
24	PIPE3XXS	24	24	24	24	24	24	24	24	24	24	24	24	24	24	24
25	PIPE6STD	25	25	25	25	25	25	25	25	25	25	25	25	25	25	25
26	PIPE5XS	26	26	26	26	26	26	26	26	26	26	26	26	26	26	26
27	PIPE4XXS	27	27	27	27	27	27	27	27	27	27	27	27	27	27	27
28	PIPE6XS	28	28	28	28	28	28	28	[]	[]	[]	[]	[]	[]	[]	[]
29	PIPE8STD	29	29	29	29	29	29	29	29	29	29	29	29	29	29	29
30	PIPE5XXS	30	30	30	30	30	30	30	30	30	30	30	[]	[]	[]	[]
31	PIPE10STD	31	31	31	31	31	31	[]	[]	[]	[]	[]	[]	[]	[]	[]
32	PIPE8XS	32	32	32	32	32	32	32	32	32	32	32	32	32	32	32
33	PIPE12STD	33	33	33	[]	[]	[]	[]	[]	[]	[]	[]	[]	[]	[]	[]
34	PIPE6XXS	[]	[]	[]	[]	[]	[]	[]	[]	[]	[]	[]	[]	[]	[]	[]
35	PIPE10XS	[]	[]	[]	[]	[]	[]	[]	[]	[]	[]	[]	[]	[]	[]	[]
36	PIPE12XS	[]	[]	[]	[]	[]	[]	[]	[]	[]	[]	[]	[]	[]	[]	[]
37	PIPE8XXS	[]	[]	[]	[]	[]	[]	[]	[]	[]	[]	[]	[]	[]	[]	[]

*[]: The final design does not contain the corresponding steel section.

Table 5.4 Number of analyses to obtain the best feasible design for 1900-member grid using MS-GSS$_A$

Stage no.	MS-GSS$_A$ optimization run no.									
	1	2	3	4	5	6	7	8	9	10
1	277	272	340	346	397	374	406	319	479	275
2	481	271	212	296	496	383	326	312	229	295
3	371	294	312	261	419	460	495	498	263	294
4	211	293	312	395	417	269	464	401	291	321
5	262	310	331	265	430	420	331	421	290	467
6	437	379	216	500	497	217	456	383	274	230
7	205	226	499	334	386	338	379	384	381	500
8	431	387	499	464	399	172	440	462	306	436
9	475	405	206	457	498	428	141	450	325	444
10	464	393	487	458	273	323	314	354	466	357
11	466	242	443	375	223	194	109	462	346	473
12	477	370	240	258	493	437	270	302	478	324
13	320	462	477	361	495	488	255	313	423	377
14	347	499	173	389	343	369	491	329	194	268
15	248	387	202	450	376	372	449	292	366	234

Table 5.5 Number of analyses to obtain the best feasible design for 1900-member grid using MS-GSS$_B$

Stage no.	MS-GSS$_B$ optimization run no.									
	1	2	3	4	5	6	7	8	9	10
1	184	221	336	164	276	248	308	206	357	349
2	312	220	229	364	356	222	362	411	392	262
3	234	437	212	493	363	369	221	209	213	490
4	208	269	442	468	500	486	331	421	277	369
5	452	182	338	411	293	425	234	446	374	413
6	500	393	435	312	432	250	209	500	383	265
7	356	440	428	465	484	287	498	425	250	424
8	498	255	217	468	420	272	209	427	488	500
9	495	282	500	418	268	445	464	394	178	245
10	281	404	409	286	479	349	262	375	452	479
11	459	425	455	489	211	243	283	216	356	239
12	439	328	241	233	368	349	402	225	229	182
13	244	445	183	266	224	500	455	315	493	270
14	249	184	200	453	256	497	324	319	487	195
15	375	197	438	342	205	227	397	445	221	408

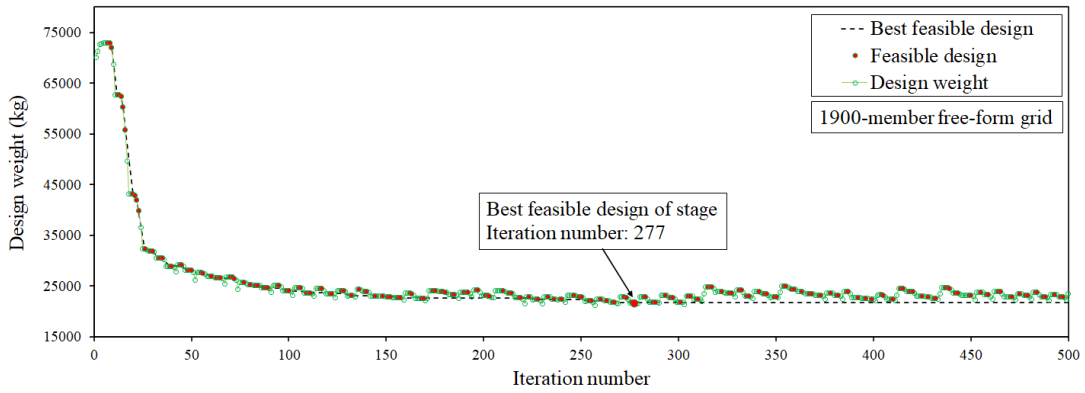

(a)

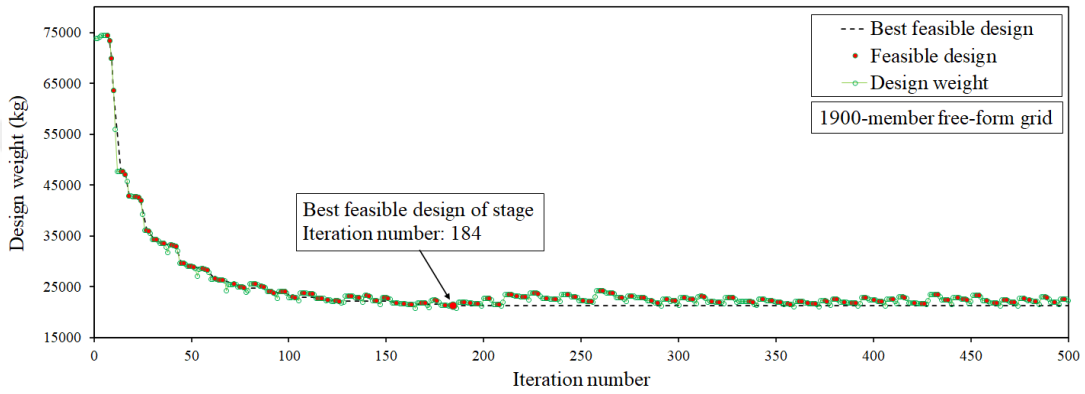

(b)

Figure 5.2 Convergence history of optimization for 1900-member free-form grid: (a) MS-GSS$_A$, (b) MS-GSS$_B$

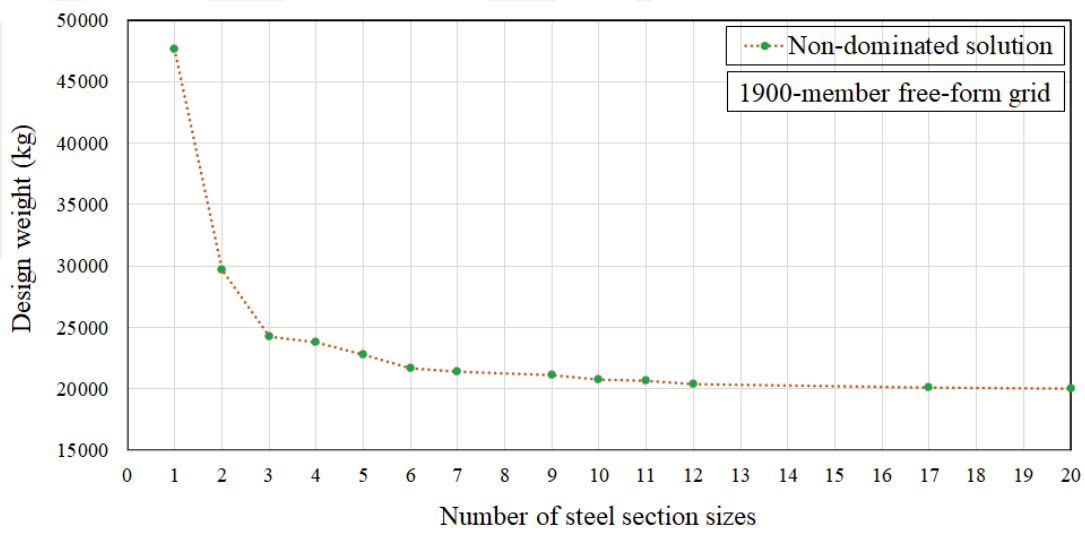

Figure 5.3 Pareto front showing the trade-off between weight and number of steel section sizes for 1900-member free-form grid

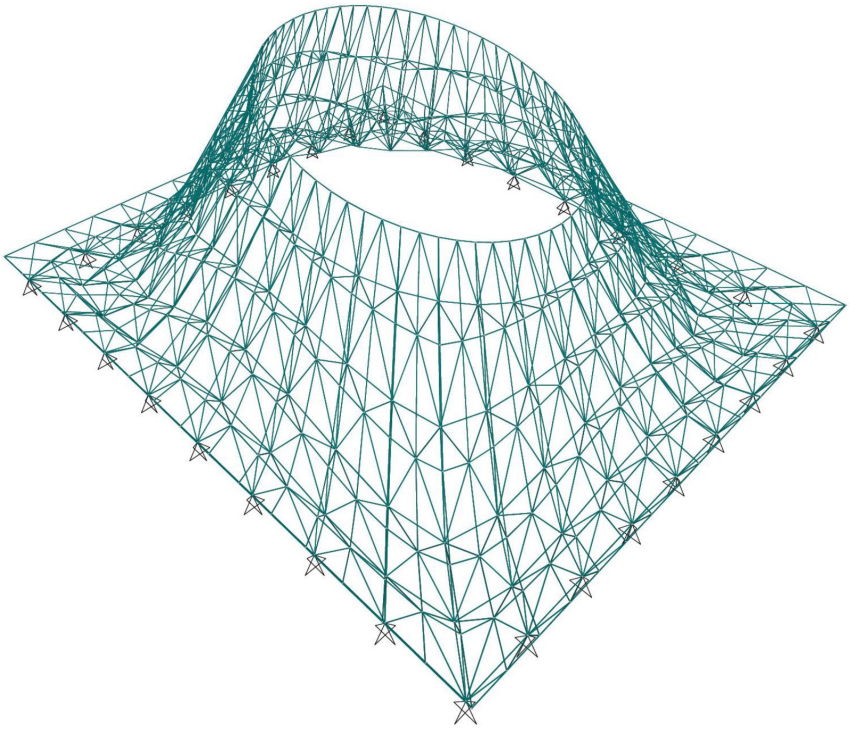

(a) perspective view

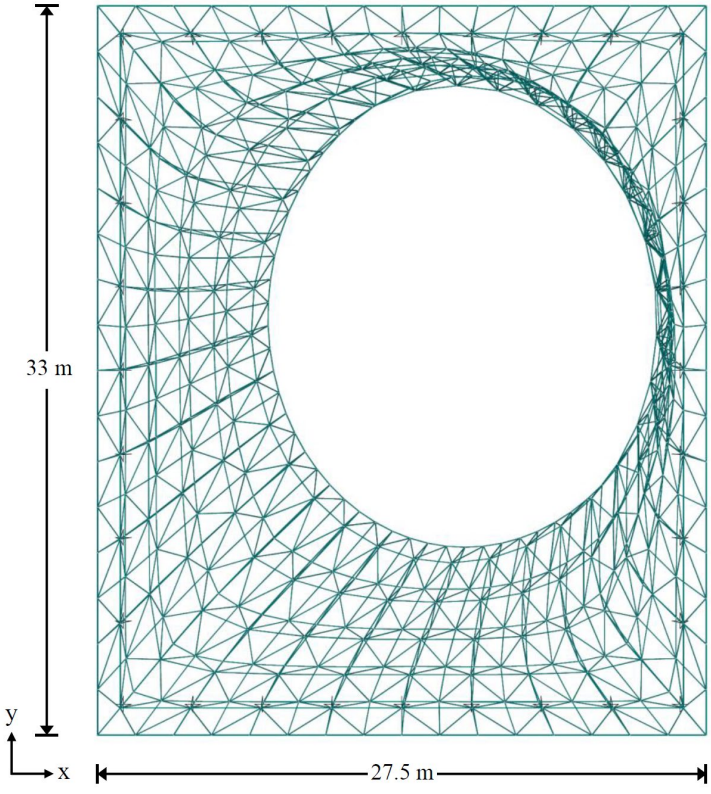

(b) plan view

Figure 5.4 1952-member free-form grid: (a) perspective view, and (b) plan view

5.1.2 Test Example 2: 1952-Member Free-Form Grid

The 1952-member double-layer grid shown in Figure 5.4 is adopted as the second test instance. The free-form grid is composed of 1952 structural elements and 544 joints. As mentioned before, although in the case of structures having regular geometrical configurations it could be possible to reduce the number of solution variables through initial member grouping, this would be cumbersome for irregularly curved free-form structures. Accordingly, discrete sizing optimization of the 1952-member free-form grid is carried out without member grouping that produces a test instance having 1952 discrete design variables. For design purpose, concentrated loads are applied at all unsupported joints of the grid in the following three cases: (i) horizontal loads of 14 kN acting in the positive x-direction, (ii) horizontal loads of 14 kN acting in the positive y-direction, and (iii) vertical loads of 14 kN acting in the negative z-direction. The 1952-member free-form grid shall be designed such that the maximum displacement of all joints in the x, y, and z directions does not exceed 2.5 cm under the above-mentioned loading conditions.

Discrete sizing optimization of the 1952-member double-layer grid is carried out over multiple stages using the MS-GSS_A and MS-GSS_B algorithms where at each stage the algorithms are allowed to utilize an updated subset of the complete set of available steel sections. Table 5.6 indicates the steel sections used in the final designs for the initial fifteen stages of the first multi-stage run of the MS-GSS_B algorithm. In the foregoing multi-stage run, at the end of the first stage, steel section number 21, namely PIPE2-1/2XXS, is found to be the most utilized profile in the best design whereas section number 2, namely PIPE1/2XS is detected as a redundant section with an insignificant contribution of 41.24 kg to the total weight of the corresponding best feasible design that is 52090.77 kg. On the other hand, as can be seen from Table 5.6, since at the end of the first stage the best feasible design obtained includes all the 37 pipe sections, only PIPE1/2XS will be eliminated from the list of available profiles before the second stage of the associated multi-stage run. Figure 5.5 shows the optimization histories for the 1952-member free-form grid, in the first stage of the first multi-stage run, using the MS-GSS_A and MS-GSS_B algorithms. As depicted in the

figure, MS-GSS$_A$ and MS-GSS$_B$ obtain the best feasible design in the above-mentioned optimization stage after 368 and 474 iterations, respectively.

Table 5.6 Multi-stage elimination of redundant sections for 1952-member grid via MS-GSS$_B$

Designation		MS-GSS$_B$ optimization stage no.														
		1	2	3	4	5	6	7	8	9	10	11	12	13	14	15
1	PIPE1/2STD	1	1	1	1	1	[]*	[]	[]	[]	[]	[]	[]	[]	[]	[]
2	PIPE1/2XS	2	[]	[]	[]	[]	[]	[]	[]	[]	[]	[]	[]	[]	[]	[]
3	PIPE3/4STD	3	3	[]	[]	[]	[]	[]	[]	[]	[]	[]	[]	[]	[]	[]
4	PIPE3/4XS	4	4	4	4	[]	[]	[]	[]	[]	[]	[]	[]	[]	[]	[]
5	PIPE1STD	5	5	5	5	5	5	5	5	5	5	5	5	5	5	5
6	PIPE1XS	6	6	6	6	6	6	6	6	[]	[]	[]	[]	[]	[]	[]
7	PIPE1-1/4STD	7	7	7	7	7	7	7	7	7	7	7	7	7	7	[]
8	PIPE1-1/2STD	8	8	8	8	8	8	8	8	8	8	[]	[]	[]	[]	[]
9	PIPE1-1/4XS	9	9	9	9	9	9	9	9	9	9	9	9	9	9	9
10	PIPE1-1/2XS	10	10	10	10	10	10	10	10	10	10	10	10	10	10	10
11	PIPE2STD	11	11	11	11	11	11	11	11	11	11	11	11	11	11	11
12	PIPE2XS	12	12	12	12	12	12	12	12	12	12	12	12	12	12	12
13	PIPE2-1/2STD	13	13	13	13	13	13	13	13	13	13	13	13	13	13	13
14	PIPE3STD	14	14	14	14	14	14	14	14	14	14	14	14	14	14	14
15	PIPE2-1/2XS	15	15	15	15	15	15	15	15	15	15	15	15	15	15	15
16	PIPE2XXS	16	16	16	16	16	16	16	16	16	16	16	16	16	16	16
17	PIPE3-1/2STD	17	17	17	17	17	17	17	17	17	17	17	17	17	17	17
18	PIPE3XS	18	18	18	18	18	18	18	18	18	18	18	18	18	18	18
19	PIPE4STD	19	19	19	19	19	19	19	19	19	19	19	19	19	19	19
20	PIPE3-1/2XS	20	20	20	20	20	20	20	20	20	20	20	20	20	20	20
21	PIPE2-1/2XXS	21	21	21	21	21	21	21	21	21	21	21	21	21	21	21
22	PIPE5STD	22	22	22	22	22	22	22	22	22	22	22	22	22	22	22
23	PIPE4XS	23	23	23	23	23	23	23	23	23	23	23	23	23	23	23
24	PIPE3XXS	24	24	24	24	24	24	24	24	24	24	24	24	24	24	24
25	PIPE6STD	25	25	25	25	25	25	25	25	25	25	25	25	25	25	25
26	PIPE5XS	26	26	26	26	26	26	26	26	26	26	26	26	26	26	26
27	PIPE4XXS	27	27	27	27	27	27	27	27	27	27	27	27	27	27	27
28	PIPE6XS	28	28	28	28	28	28	28	28	28	28	28	28	28	[]	[]
29	PIPE8STD	29	29	29	29	29	29	29	29	29	29	29	29	[]	[]	[]
30	PIPE5XXS	30	30	30	30	30	30	30	30	30	30	30	30	30	30	30
31	PIPE10STD	31	31	31	31	31	31	31	31	31	31	31	[]	[]	[]	[]
32	PIPE8XS	32	32	32	32	32	32	[]	[]	[]	[]	[]	[]	[]	[]	[]
33	PIPE12STD	33	33	33	33	33	33	33	[]	[]	[]	[]	[]	[]	[]	[]
34	PIPE6XXS	34	34	34	[]	[]	[]	[]	[]	[]	[]	[]	[]	[]	[]	[]
35	PIPE10XS	35	35	35	35	35	35	[]	[]	[]	[]	[]	[]	[]	[]	[]
36	PIPE12XS	36	36	36	36	36	36	36	36	36	[]	[]	[]	[]	[]	[]
37	PIPE8XXS	37	37	37	37	37	37	37	37	37	37	37	37	37	37	37

*[]: The final design does not contain the corresponding steel section.

It is worthwhile to note that computational efficiency of the employed algorithms facilitates multiple optimization stages of challenging test cases in a timely manner. Table 5.7 provides the number of structural analyses to locate the best feasible solution for the 1952-member grid over the initial fifteen stages of the first multi-stage run using the MS-GSS$_B$ algorithm. Moreover, to illustrate the trade-off between weight and number of employed steel section sizes, the non-dominated solutions obtained using the MS-GSS$_A$ and MS-GSS$_B$ algorithms are presented in Figure 5.6.

Table 5.7 Number of analyses to obtain the best feasible design for 1952-member grid using MS-GSS$_B$

Stage no.	MS-GSS$_B$ optimization run no.									
	1	2	3	4	5	6	7	8	9	10
1	474	293	407	462	457	274	496	422	405	469
2	397	425	476	404	334	346	419	371	377	348
3	404	474	443	400	474	347	409	477	470	471
4	500	323	266	467	152	462	483	491	412	403
5	359	374	372	486	397	323	380	336	398	455
6	329	450	242	499	195	485	213	362	331	456
7	371	473	470	292	484	394	388	465	382	372
8	485	497	260	464	451	277	471	203	467	448
9	410	336	490	463	306	381	476	352	271	393
10	401	500	303	449	211	454	238	430	381	343
11	332	275	347	319	153	311	324	426	303	438
12	298	437	202	469	388	460	261	382	422	481
13	446	226	459	408	426	461	152	403	496	186
14	306	356	443	256	152	322	380	123	420	466
15	122	360	308	206	468	427	111	484	361	309

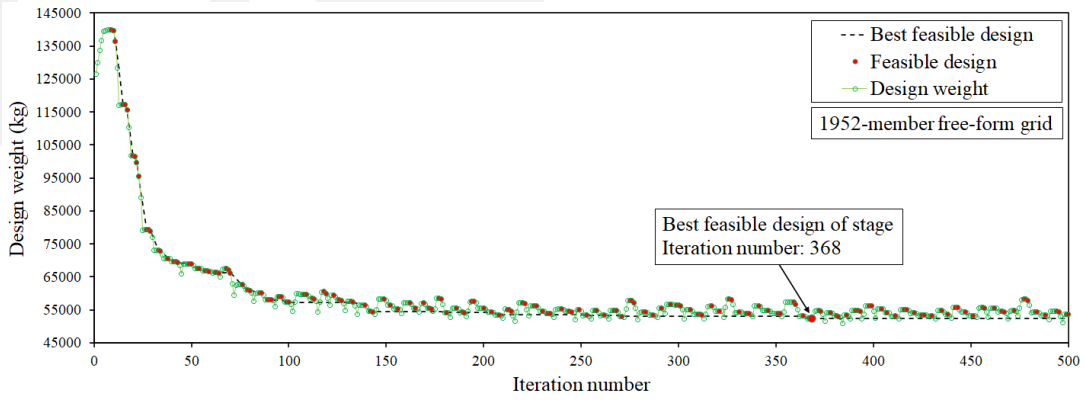

(a)

Figure 5.5 Convergence history of optimization for 1952-member free-form grid: (a) MS-GSS$_A$, (b) MS-GSS$_B$

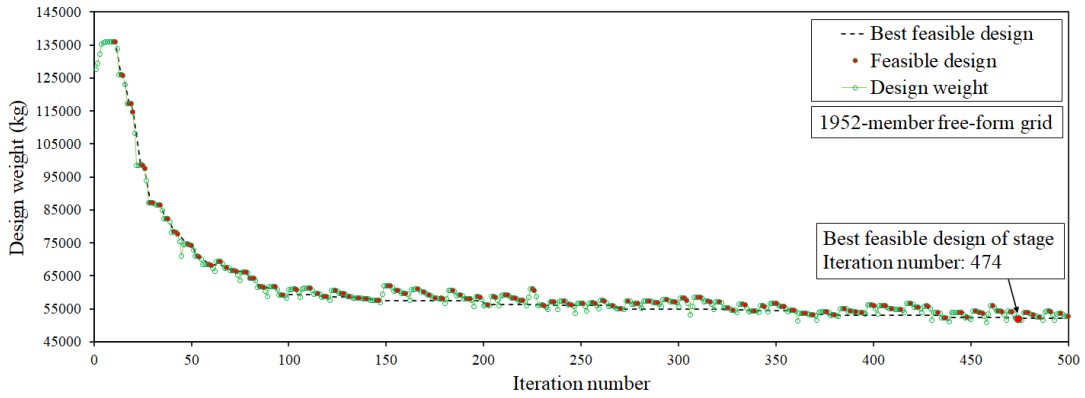

(b)

Figure 5.5 (continued)

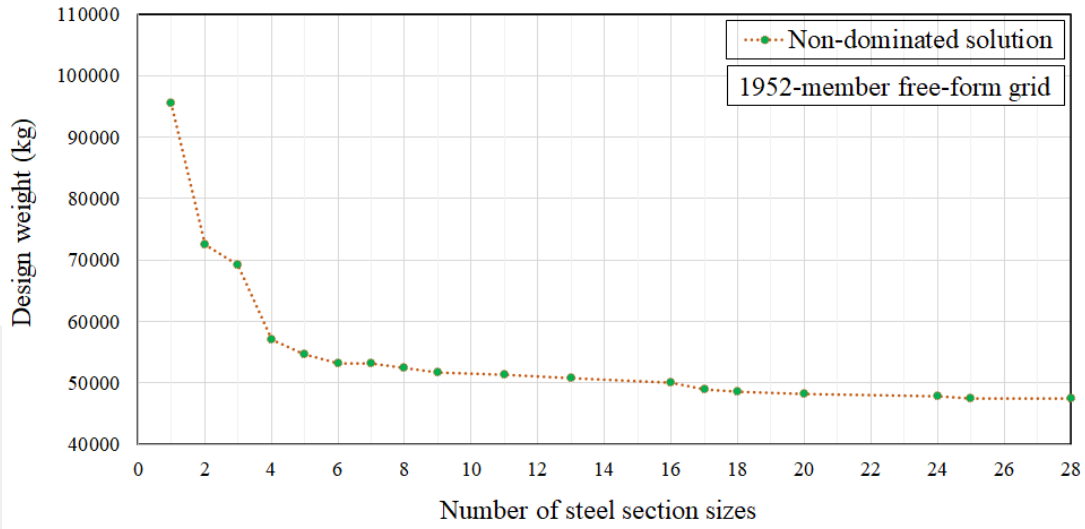

Figure 5.6 Pareto front showing the trade-off between weight and number of steel section sizes for 1952-member free-form grid

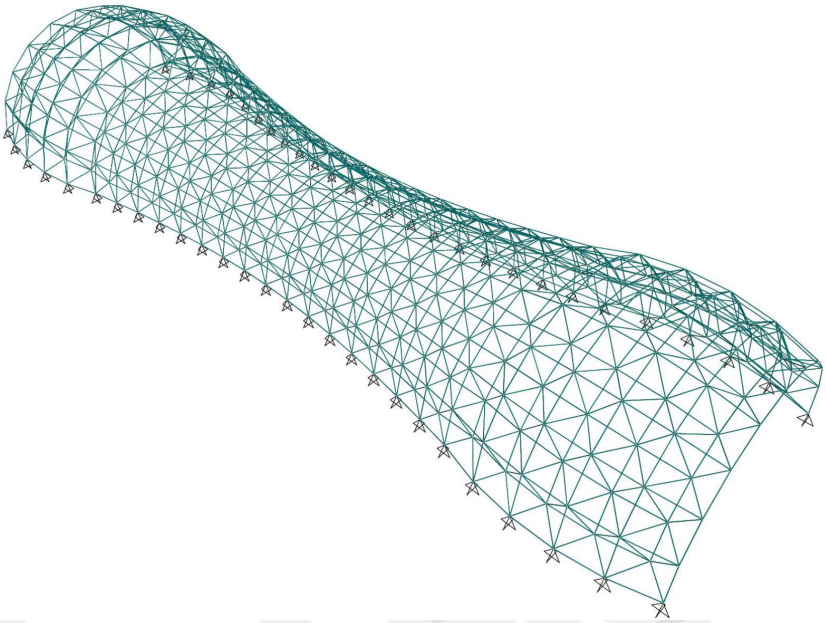

(a) perspective view

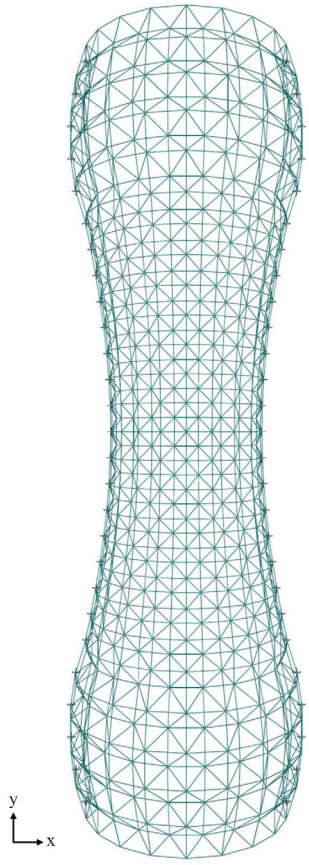

(b) plan view

Figure 5.7 2080-member free-form grid: (a) perspective view, and (b) plan view

5.1.3 Test Example 3: 2080-Member Free-Form Grid

Multi-stage discrete sizing optimization of the 2080-member double-layer grid shown in Figure 5.7 is carried out in this test example. The free-form grid is 64 m long with varying width and height and comprises 2080 structural members and 557 joints. Since no member grouping is performed, the design optimization problem includes 2080 discrete sizing design variables. To generate the geometric configuration of the free-form grid, the parametric formex formulation provided in [6] is used with some adjustments to the associated parameters. The free-form double-layer grid shall be designed to sustain the following three independent loading cases. Here, concentrated loads are applied at all the unsupported joints of the free-form double-layer grid in the following cases: (i) horizontal loads of 15 kN acting in the positive x-direction, (ii) horizontal loads of 15 kN acting in the positive y-direction, and (iii) vertical loads of 15 kN acting in the negative z-direction. Moreover, the maximum displacement of all joints of the 2080-member free-form grid in the x, y, and z directions is limited to 5 cm.

Multi-stage design optimization of the 2080-member free-form grid is performed using the MS-GSS_A and MS-GSS_B algorithms where in the first stage, the complete set of available steel sections is introduced to the algorithms. Table 5.8 shows the contribution of different steel section sizes to the total weight of the best feasible design, namely 59754.16 kg, obtained at the end of the first stage of the first multi-stage run of the MS-GSS_A algorithm. As can be seen from the table, steel section number 24, namely PIPE3XXS, is the most utilized profile in the best feasible design that forms 6.1% of the total weight of the design. On the other hand, steel section number 2, i.e., PIPE1/2XS is the least utilized steel section with 0.06% contribution to the total design weight. As a result, at the end of the first stage, PIPE1/2XS is identified as a redundant section which will be removed from the list of available profiles. Table 5.9 presents the utilized sections in the final design of each stage for the first multi-stage run of the MS-GSS_A algorithm. Akin to the previous examples, for the sake of brevity the results are given for the initial fifteen stages of the algorithm. As indicated in Table 5.9, since the obtained best feasible design at the end of the first stage includes all the 37 pipe sections, as a redundant section, only PIPE1/2XS will be removed from

Table 5.8 Contribution of steel section sizes to the design weight of 2080-member grid using MS-GSS_A

Section no.	Designation	Area (cm^2)	Total length (m)	Total weight (kg)	% of grid weight
24	PIPE3XXS	35.2903	131.52	3643.46	6.10
27	PIPE4XXS	52.258	81.17	3329.96	5.57
21	PIPE2-1/2XXS	25.9999	161.39	3294.03	5.51
16	PIPE2XXS	17.1613	225.36	3035.93	5.08
26	PIPE5XS	39.4193	92.35	2857.70	4.78
37	PIPE8XXS	137.4191	24.73	2667.70	4.46
12	PIPE2XS	9.5484	342.70	2568.67	4.30
25	PIPE6STD	35.9999	85.40	2413.48	4.04
15	PIPE2-1/2XS	14.5161	198.86	2265.98	3.79
28	PIPE6XS	54.1934	52.97	2253.57	3.77
31	PIPE10STD	76.774	36.45	2196.96	3.68
13	PIPE2-1/2STD	10.9677	229.41	1975.10	3.31
23	PIPE4XS	28.4516	88.30	1972.17	3.30
11	PIPE2STD	6.9032	351.73	1906.02	3.19
29	PIPE8STD	54.1934	44.69	1901.22	3.18
18	PIPE3XS	19.4838	123.72	1892.31	3.17
10	PIPE1-1/2XS	6.9032	331.32	1795.45	3.00
35	PIPE10XS	103.8708	20.98	1710.74	2.86
19	PIPE4STD	20.4516	92.92	1491.72	2.50
22	PIPE5STD	27.7419	62.13	1353.14	2.26
17	PIPE3-1/2STD	17.2903	96.47	1309.37	2.19
20	PIPE3-1/2XS	23.7419	68.01	1267.52	2.12
14	PIPE3STD	14.3871	108.48	1225.19	2.05
30	PIPE5XXS	72.9031	20.77	1188.53	1.99
36	PIPE12XS	123.8707	11.99	1166.21	1.95
34	PIPE6XXS	100.645	14.35	1133.77	1.90
32	PIPE8XS	82.5805	15.99	1036.77	1.74
8	PIPE1-1/2STD	5.1548	228.28	923.72	1.55
9	PIPE1-1/4XS	5.6839	206.13	919.74	1.54
33	PIPE12STD	94.1934	11.73	867.08	1.45
6	PIPE1XS	4.1226	183.55	594.00	0.99
7	PIPE1-1/4STD	4.3161	171.47	580.98	0.97
1	PIPE1/2STD	1.6129	327.57	414.74	0.69
5	PIPE1STD	3.1871	110.44	276.32	0.46
4	PIPE3/4XS	2.7935	77.95	170.95	0.29
3	PIPE3/4STD	2.1484	69.70	117.55	0.20
2	PIPE1/2XS	2.0645	22.48	36.44	0.06
Total				59754.16	100

Table 5.9 Multi-stage elimination of redundant sections for 2080-member grid via MS-GSS$_A$

Designation		MS-GSS$_A$ optimization stage no.														
		1	2	3	4	5	6	7	8	9	10	11	12	13	14	15
1	PIPE1/2STD	1	1	1	1	1	1	1	1	1	[]*	[]	[]	[]	[]	[]
2	PIPE1/2XS	2	[]	[]	[]	[]	[]	[]	[]	[]	[]	[]	[]	[]	[]	[]
3	PIPE3/4STD	3	3	[]	[]	[]	[]	[]	[]	[]	[]	[]	[]	[]	[]	[]
4	PIPE3/4XS	4	4	4	4	[]	[]	[]	[]	[]	[]	[]	[]	[]	[]	[]
5	PIPE1STD	5	5	5	5	5	5	[]	[]	[]	[]	[]	[]	[]	[]	[]
6	PIPE1XS	6	6	6	6	6	6	6	6	6	6	6	6	6	6	6
7	PIPE1-1/4STD	7	7	7	7	7	7	7	7	[]	[]	[]	[]	[]	[]	[]
8	PIPE1-1/2STD	8	8	8	8	8	8	8	8	8	8	8	[]	[]	[]	[]
9	PIPE1-1/4XS	9	9	9	9	9	9	9	9	9	9	9	9	9	9	9
10	PIPE1-1/2XS	10	10	10	10	10	10	10	10	10	10	10	10	10	10	10
11	PIPE2STD	11	11	11	11	11	11	11	11	11	11	11	11	11	11	11
12	PIPE2XS	12	12	12	12	12	12	12	12	12	12	12	12	12	12	12
13	PIPE2-1/2STD	13	13	13	13	13	13	13	13	13	13	13	13	13	13	13
14	PIPE3STD	14	14	14	14	14	14	14	14	14	14	14	14	[]	[]	[]
15	PIPE2-1/2XS	15	15	15	15	15	15	15	15	15	15	15	15	15	15	15
16	PIPE2XXS	16	16	16	16	16	16	16	16	16	16	16	16	16	16	16
17	PIPE3-1/2STD	17	17	17	17	17	17	17	17	17	17	17	17	17	17	17
18	PIPE3XS	18	18	18	18	18	18	18	18	18	18	18	18	18	18	18
19	PIPE4STD	19	19	19	19	19	19	19	19	19	19	19	19	19	19	19
20	PIPE3-1/2XS	20	20	20	20	20	20	20	20	20	20	20	20	20	20	20
21	PIPE2-1/2XXS	21	21	21	21	21	21	21	21	21	21	21	21	21	21	21
22	PIPE5STD	22	22	22	22	22	22	22	22	22	22	22	22	22	22	22
23	PIPE4XS	23	23	23	23	23	23	23	23	23	23	23	23	23	23	23
24	PIPE3XXS	24	24	24	24	24	24	24	24	24	24	24	24	24	24	24
25	PIPE6STD	25	25	25	25	25	25	25	25	25	25	25	25	25	25	25
26	PIPE5XS	26	26	26	26	26	26	26	26	26	26	26	26	26	26	26
27	PIPE4XXS	27	27	27	27	27	27	27	27	27	27	27	27	27	27	27
28	PIPE6XS	28	28	28	28	28	28	28	28	28	28	28	28	28	28	28
29	PIPE8STD	29	29	29	29	29	29	29	29	29	29	29	29	29	29	29
30	PIPE5XXS	30	30	30	30	30	30	30	30	30	30	30	30	30	30	30
31	PIPE10STD	31	31	31	31	31	31	31	31	31	31	31	31	31	[]	[]
32	PIPE8XS	32	32	32	32	32	32	32	32	32	32	[]	[]	[]	[]	[]
33	PIPE12STD	33	33	33	33	33	33	33	[]	[]	[]	[]	[]	[]	[]	[]
34	PIPE6XXS	34	34	34	34	34	[]	[]	[]	[]	[]	[]	[]	[]	[]	[]
35	PIPE10XS	35	35	35	35	35	35	35	35	35	35	35	35	35	35	[]
36	PIPE12XS	36	36	36	[]	[]	[]	[]	[]	[]	[]	[]	[]	[]	[]	[]
37	PIPE8XXS	37	37	37	37	37	37	37	37	37	37	37	37	37	37	37

*[]: The final design does not contain the corresponding steel section.

the list of available profiles before the next optimization stage. It is important to note that, in general, the elimination sequence of redundant sections could change over different multi-stage runs due to the stochastic nature of the employed optimization techniques. Figure 5.8 shows the Pareto front composed of non-dominated designs obtained for the 2080-member free-form grid and illustrates the trade-off between weight and number of employed steel section sizes.

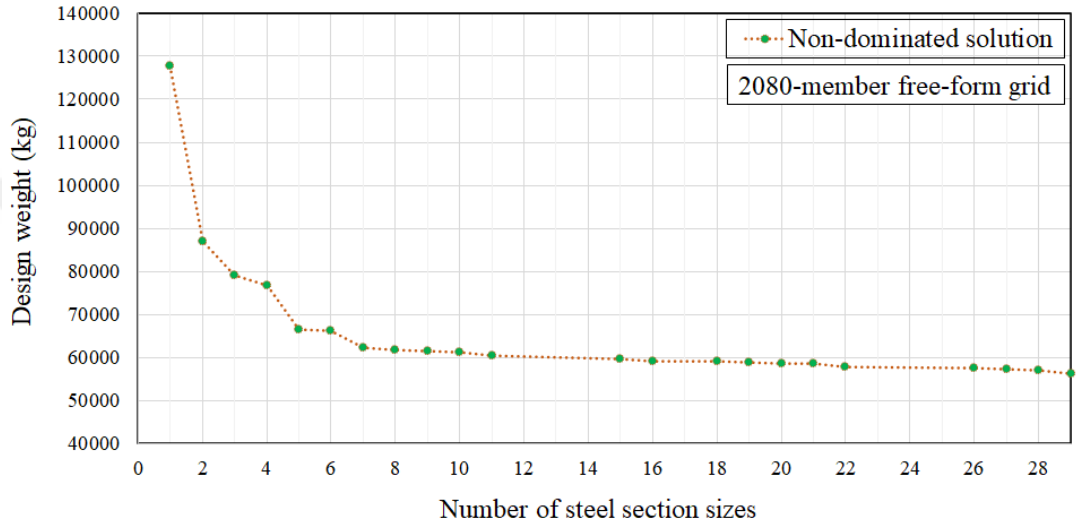

Figure 5.8 Pareto front showing the trade-off between weight and number of steel section sizes for 2080-member free-form grid

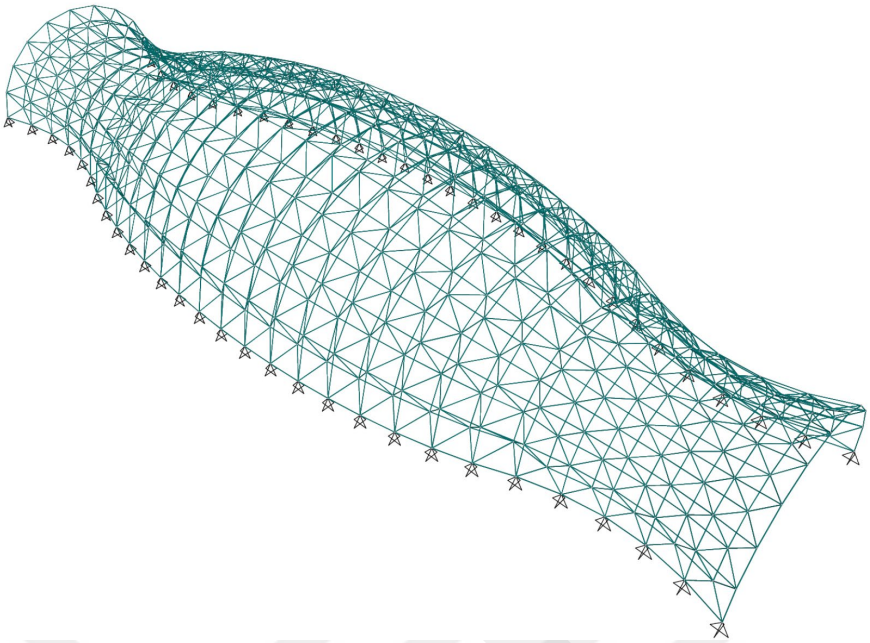

(a) perspective view

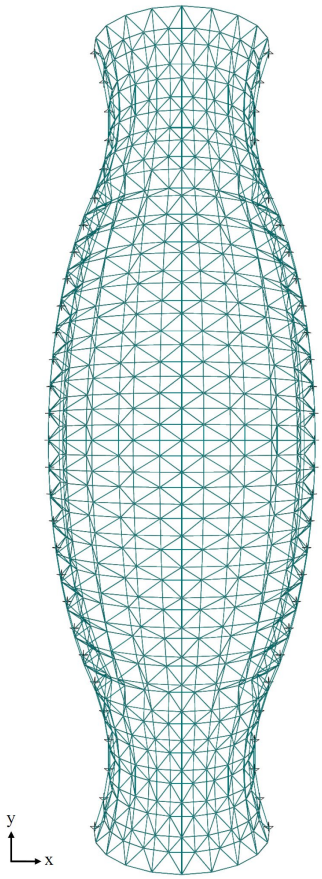

(b) plan view

Figure 5.9 2240-member free-form grid: (a) perspective view, and (b) plan view

5.1.4 Test Example 4: 2240-Member Free-Form Grid

To investigate the trade-off between weight and number of different section sizes in the final design, the 2240-member double-layer grid shown in Figure 5.9 is selected as the last test instance. The structure is 64 m long with varying width and height and consists of 2240 structural elements and 599 joints. Akin to the previous examples, since no member grouping is carried out, the design optimization problem involves 2240 distinct design variables. To Develop the geometric configuration of the grid, the generic formex formulation presented in [6] is utilized with some adjustments to the corresponding parameters. For design purpose, concentrated loads are applied at all the unsupported joints of the free-form double-layer grid in the following loading cases: (i) horizontal loads of 12 kN acting in the positive x-direction, (ii) horizontal loads of 12 kN acting in the positive y-direction, and (iii) vertical loads of 16 kN acting in the negative z-direction. The 2240-member free-form grid shall be designed such that under the above-mentioned loading cases the maximum displacement of all joints in the x, y, and z directions does not exceed 2.5 cm.

Optimization of the 2240-member free-form grid is carried out over multiple stages using the MS-GSS_A and MS-GSS_B algorithms where at each stage the algorithms are allowed to use an updated subset of the complete set of available steel sections. Table 5.10 indicates the steel sections used in the final designs for the initial fifteen stages of the first multi-stage run of the MS-GSS_B algorithm. In the foregoing multi-stage run, at the end of the first stage, steel section number 21, namely PIPE2-1/2XXS, is found to be the most utilized profile in the best design whereas section number 2, namely PIPE1/2XS is detected as the redundant section with an insignificant contribution of 27.04 kg to the total weight of the corresponding best feasible design that is 63226.18 kg. Considering that in the investigated test examples RS parameter is set to 1, at the end of each stage at least one section size is to be eliminated from the remaining subset of steel sections. For instance, as can also be observed from Table 5.10, at the end of stages 1, 2, 3, 4, and 5, PIPE1/2XS, PIPE3/4STD, PIPE3/4XS, PIPE1STD, and PIPE1/2STD are eliminated from the remaining profile list, respectively. Consequently, stage 6 of optimization is started using a subset of 32 pipe sections from

which PIPE12XS is not used in the corresponding best feasible design. The remaining optimization stages are performed in a similar manner as already described.

Table 5.10 Multi-stage elimination of redundant sections for 2240-member grid via MS-GSS$_B$

Designation		MS-GSS$_B$ optimization stage no.														
		1	2	3	4	5	6	7	8	9	10	11	12	13	14	15
1	PIPE1/2STD	1	1	1	1	1	[]*	[]	[]	[]	[]	[]	[]	[]	[]	[]
2	PIPE1/2XS	2	[]	[]	[]	[]	[]	[]	[]	[]	[]	[]	[]	[]	[]	[]
3	PIPE3/4STD	3	3	[]	[]	[]	[]	[]	[]	[]	[]	[]	[]	[]	[]	[]
4	PIPE3/4XS	4	4	4	[]	[]	[]	[]	[]	[]	[]	[]	[]	[]	[]	[]
5	PIPE1STD	5	5	5	5	[]	[]	[]	[]	[]	[]	[]	[]	[]	[]	[]
6	PIPE1XS	6	6	6	6	6	6	6	6	6	6	6	6	6	6	6
7	PIPE1-1/4STD	7	7	7	7	7	7	7	7	7	7	7	[]	[]	[]	[]
8	PIPE1-1/2STD	8	8	8	8	8	8	8	8	[]	[]	[]	[]	[]	[]	[]
9	PIPE1-1/4XS	9	9	9	9	9	9	9	9	9	9	9	9	9	9	9
10	PIPE1-1/2XS	10	10	10	10	10	10	10	10	10	10	10	10	10	10	10
11	PIPE2STD	11	11	11	11	11	11	11	11	11	11	11	11	11	11	11
12	PIPE2XS	12	12	12	12	12	12	12	12	12	12	12	12	12	12	12
13	PIPE2-1/2STD	13	13	13	13	13	13	13	13	13	13	13	13	13	13	13
14	PIPE3STD	14	14	14	14	14	14	14	14	14	14	14	14	14	[]	[]
15	PIPE2-1/2XS	15	15	15	15	15	15	15	15	15	15	15	15	15	15	15
16	PIPE2XXS	16	16	16	16	16	16	16	16	16	16	16	16	16	16	16
17	PIPE3-1/2STD	17	17	17	17	17	17	17	17	17	17	17	17	17	17	17
18	PIPE3XS	18	18	18	18	18	18	18	18	18	18	18	18	18	18	18
19	PIPE4STD	19	19	19	19	19	19	19	19	19	19	19	19	19	19	[]
20	PIPE3-1/2XS	20	20	20	20	20	20	20	20	20	20	20	20	20	20	20
21	PIPE2-1/2XXS	21	21	21	21	21	21	21	21	21	21	21	21	21	21	21
22	PIPE5STD	22	22	22	22	22	22	22	22	22	22	22	22	22	22	22
23	PIPE4XS	23	23	23	23	23	23	23	23	23	23	23	23	23	23	23
24	PIPE3XXS	24	24	24	24	24	24	24	24	24	24	24	24	24	24	24
25	PIPE6STD	25	25	25	25	25	25	25	25	25	25	25	25	25	25	25
26	PIPE5XS	26	26	26	26	26	26	26	26	26	26	26	26	26	26	26
27	PIPE4XXS	27	27	27	27	27	27	27	27	27	27	27	27	27	27	27
28	PIPE6XS	28	28	28	28	28	28	28	28	28	28	28	28	28	28	28
29	PIPE8STD	29	29	29	29	29	29	29	29	29	[]	[]	[]	[]	[]	[]
30	PIPE5XXS	30	30	30	30	30	30	30	30	30	30	30	30	30	30	30
31	PIPE10STD	31	31	31	31	31	31	31	31	31	31	31	31	31	31	31
32	PIPE8XS	32	32	32	32	32	32	32	32	32	32	32	32	[]	[]	[]
33	PIPE12STD	33	33	33	33	33	33	33	[]	[]	[]	[]	[]	[]	[]	[]
34	PIPE6XXS	34	34	34	34	34	34	[]	[]	[]	[]	[]	[]	[]	[]	[]
35	PIPE10XS	35	35	35	35	35	35	35	35	35	35	[]	[]	[]	[]	[]
36	PIPE12XS	36	36	36	36	36	[]	[]	[]	[]	[]	[]	[]	[]	[]	[]
37	PIPE8XXS	37	37	37	37	37	37	37	37	37	37	37	37	37	37	37

*[]: The final design does not contain the corresponding steel section.

Table 5.11 Number of analyses to obtain the best feasible design for 2240-member grid using MS-GSS$_A$

Stage no.	MS-GSS$_A$ optimization run no.									
	1	2	3	4	5	6	7	8	9	10
1	298	262	411	332	221	483	264	229	444	500
2	332	404	220	380	404	474	292	221	187	357
3	228	218	438	209	332	370	462	500	425	274
4	393	453	417	497	354	285	230	338	487	163
5	453	497	256	318	221	431	428	256	396	370
6	438	291	350	412	463	400	452	283	274	367
7	187	392	292	363	192	475	288	245	383	446
8	199	300	148	484	268	224	423	477	273	493
9	444	311	299	322	493	294	349	386	249	347
10	296	254	145	491	197	362	417	271	168	489
11	443	150	431	123	458	326	459	485	381	214
12	435	331	150	251	164	427	283	166	406	234
13	398	349	225	456	140	269	264	252	121	226
14	231	465	465	227	436	103	441	474	213	184
15	265	456	131	336	223	270	438	478	329	416

Table 5.12 Number of analyses to obtain the best feasible design for 2240-member grid using MS-GSS$_B$

Stage no.	MS-GSS$_B$ optimization run no.									
	1	2	3	4	5	6	7	8	9	10
1	306	367	499	264	312	344	411	484	196	479
2	466	313	441	437	482	447	374	478	408	452
3	482	468	473	402	221	279	323	489	237	476
4	498	295	271	281	490	369	174	178	310	181
5	361	401	191	211	318	316	349	277	374	269
6	311	332	359	249	209	459	322	496	470	399
7	222	438	413	383	411	184	284	219	458	414
8	187	430	375	237	224	497	480	334	340	377
9	271	239	448	488	459	255	455	472	232	210
10	248	462	343	441	347	242	205	500	459	396
11	405	435	366	316	337	318	457	328	252	379
12	213	244	369	295	486	258	286	192	252	496
13	131	305	476	178	139	479	264	410	500	364
14	449	330	358	387	247	156	433	495	273	293
15	213	294	173	391	311	435	437	114	491	248

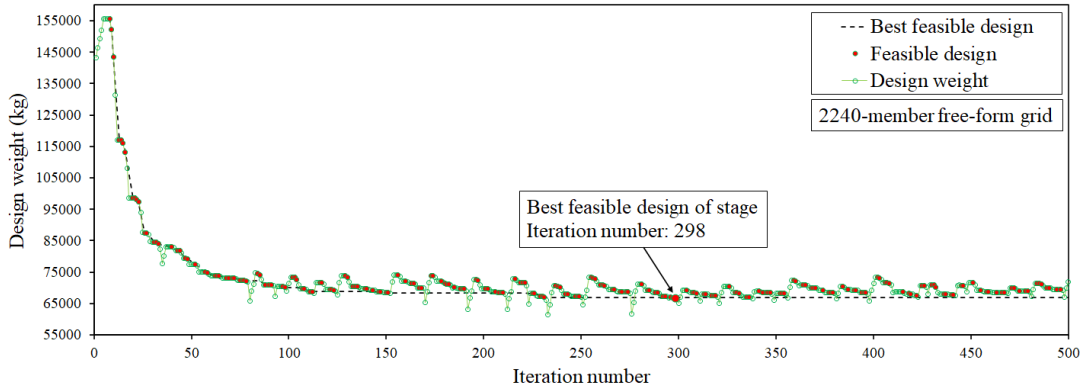

(a)

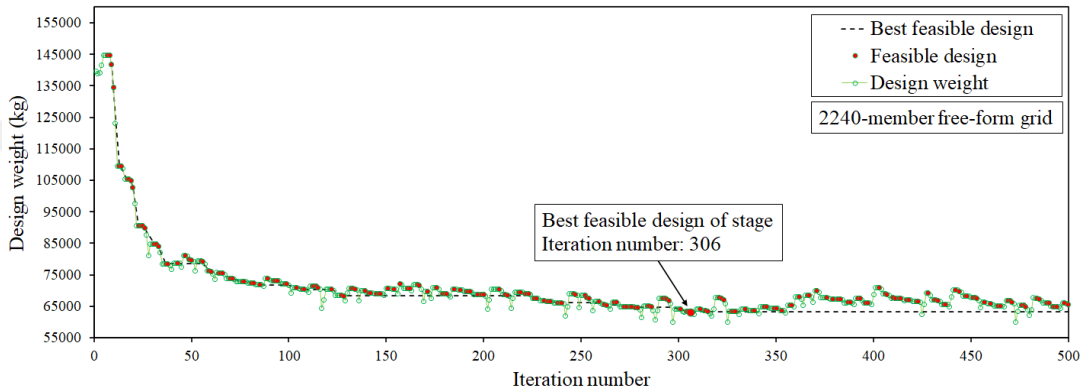

(b)

Figure 5.10 Convergence history of optimization for 2240-member free-form grid: (a) MS-GSS$_A$, (b) MS-GSS$_B$

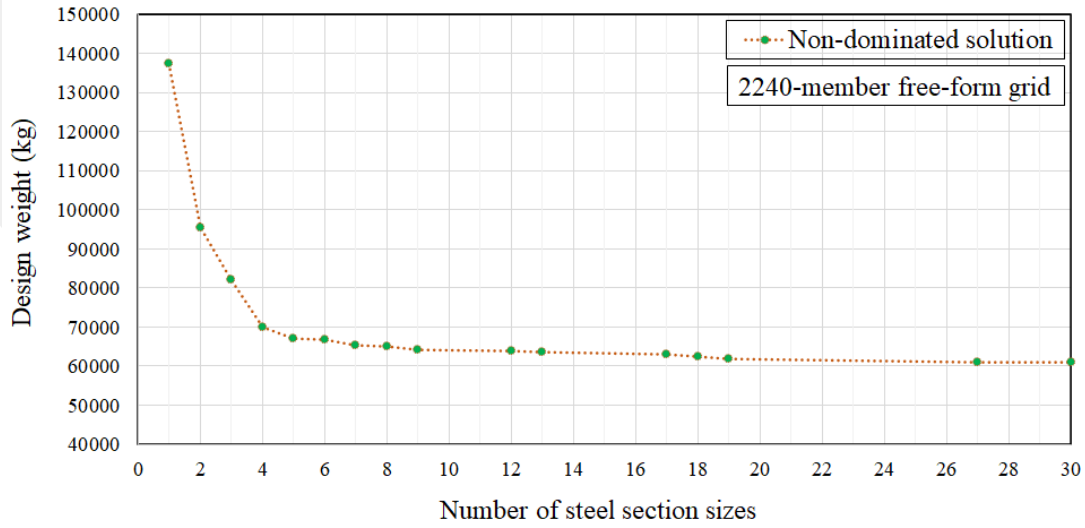

Figure 5.11 Pareto front showing the trade-off between weight and number of steel section sizes for 2240-member free-form grid

Figure 5.10 shows the convergence history of optimization for the 2240-member free-form grid, in the first stage of the first multi-stage run, using the proposed MS-GSS_A and MS-GSS_B algorithms. As depicted in the figure, MS-GSS_A and MS-GSS_B obtain the best feasible design in the above-mentioned optimization stage after 298 and 306 iterations, respectively. Tables 5.11 and 5.12 provide the number of structural analyses to obtain the best feasible design for the 2240-member free-form grid, over the initial fifteen stages of the first multi-stage run, using the MS-GSS_A and MS-GSS_B. Besides, to illustrate the trade-off between weight and number of utilized distinct section sizes, the Pareto front composed of non-dominated solutions found by the employed algorithms are presented in Figure 5.11. As already mentioned, the presented Pareto fronts can subsequently be employed by a decision-maker for optimum structural standardization considering the associated costs.

CHAPTER 6

CONCLUSIONS

6.1 Summary and Concluding Remarks

In the context of computer-aided optimization of steel skeletal structures, it is known that the obtained final designs using conventional optimization algorithms may not be necessarily favored in practice if certain provisions are not stipulated by the optimization algorithm to prevent an abundance of steel section sizes in the final design. Although grouping the structural members can limit the maximum number of distinct sections in the final design to the number of member groups, often a suitable member grouping scheme in not known prior to solving the design optimization problem. An initial intuitive member grouping based on experience and skills of the structural engineer becomes even more arduous in the case of geometrically irregular structures such as free-form steel double-layer grids where detecting similarities between members in terms of structural behavior is not trivial.

In the present thesis study, to promote the use of optimization techniques in practice, a computationally efficient multi-stage guided stochastic search (MS-GSS) method is proposed to investigate the trade-off between the number of different section sizes utilized in the final design and the minimum weight of free-form steel double-layer grids with numerous discrete variables. The proposed algorithm works on the basis of a gradual design-oriented reduction of the set of available steel profiles and repeating the optimization process using the newly updated smaller subset of the complete list of sections. Accordingly, a multi-stage run of the algorithm entails running multiple stages of design optimization where at each stage the algorithm is allowed to use an updated subset of the complete set of available steel sections. To this end, the best feasible solution obtained from the preceding optimization stage is used to identify the redundant sections for elimination. Two variants of the algorithm, i.e., MS-GSS_A and

MS-GSS$_B$ are employed to indicate the usefulness of the proposed methodology in large-scale test instances of free-form steel double-layer grids, namely a 1900-member free-form grid, a 1952-member free-form grid, a 2080-member free-form grid, and a 2240-member free-form grid, and the obtained Pareto fronts illustrating the trade-off between weight and number of distinct steel section sizes are elaborated. The provided Pareto fronts can readily be used by a decision-maker for optimum structural standardization with respect to the associated costs such as bulk purchasing or overall construction costs.

6.2 Recommendations for Future Research

In terms of design variables, although the present study is limited to discrete sizing optimization of free-form steel double-layer grids, further research can be carried out to include shape (geometry) and topology design variables in the course of optimization. Moreover, optimization and standardization of free-form double-layer grids considering more realistic design load combinations stipulated by standard design codes could be fruitful. Finally, it is also worth mentioning that developing software, with suitable graphical user interfaces (GUIs), for optimization and standardization of complex structural systems can further promote the use of optimization algorithms in practice.

REFERENCES

[1] A. Koronaki, P. Shepherd, and M. Evernden, "Rationalization of freeform space-frame structures: Reducing variability in the joints," *International Journal of Architectural Computing*, vol. 18, no. 1, pp. 84-99, 2020.

[2] H. Nooshin, and P. Disney, "Formex Configuration Processing I," *International Journal of Space Structures*, vol. 15, no. 1, pp. 1-52, 2000.

[3] H. Nooshin, P. Disney, "Formex Configuration Processing II, Int J Space Struct," vol. 16, no. 1, pp. 1-56, 2001.

[4] H. Nooshin, and P. Disney, "Formex Configuration Processing III," *International Journal of Space Structures*, vol. 17, no. 1, pp. 1-50, 2002.

[5] H. Nooshin, R. Kamyab, and O.A. Samavati, "Exploring scallop forms," *International Journal of Space Structures*, vol. 32, no. 2, pp. 84-111, 2017.

[6] M. Moghimi, "Formex configuration processing of compound and freeform structures," Ph.D. dissertation, University of Surrey, UK, 2006.

[7] H. Nooshin, and M. Moghimi, "Formex formulation of freeform structural surfaces," *Asian Journal of Civil Engineering*, vol. 8, no. 4, pp. 459-469, 2007.

[8] B. Gao, C. Hao, T. Li, and J. Ye, "Grid generation on free-form surface using guide line advancing and surface flattening method," *Advances in Engineering Software*, vol. 110, pp. 98-109, 2017.

[9] B. Gao, T. Li, T. Ma, J. Ye, J. Becque, and I. Hajirasouliha, "A practical grid generation procedure for the design of free-form structures," *Computers & Structures*, vol. 196, pp. 292-310, 2018.

[10] T. Li, J. Ye, P. Shepherd, H. Wu, and B. Gao, "Computational grid generation for the design of free-form shells with complex boundary conditions," *Journal of Computing in Civil Engineering*, vol. 33, no. 3, pp. 04019004, 2019.

[11] F. Liu, R. Feng, and K.D. Tsavdaridis, "A novel progressive grid generation method for free-form grid structure design and case studies," *Journal of Building Engineering*, vol. 34, pp. 101866, 2021.

[12] F. Erbatur, and M.M. Al-Hussainy, "Optimum design of frames," *Computers & Structures*, vol. 45, pp. 887-891, 1992.

[13] E.I. Tabak, and P.M. Wright, "Optimality criteria method for building frames," *Journal of the Structural Division*, ASCE, vol. 107, no. 7, pp. 1327-1342, 1981.

[14] M.P. Saka, "Optimum design of pin-jointed steel structures with practical applications," *Journal of Structural Engineering*, ASCE, vol. 116, no. 10, pp. 2599-2620, 1990.

[15] L. Lamberti, and C. Pappalettere, (2011) "Metaheuristic design optimization of skeletal structures: a review," in *Computational Technology Reviews*, Y. Tsompanakis, and B.H.V. Topping, Eds. Stirlingshire: Saxe-Coburg Publications, 2011, pp. 1-32.

[16] M.P. Saka, "Optimum design of steel frames using stochastic search techniques based on natural phenomena: a review," in *Civil Engineering Computations: Tools and Techniques*, B.H.V. Topping, Ed. Stirlingshire: Saxe-Coburg Publications, 2007, pp. 105-147.

[17] V. Togan, and A.T. Daloglu, "An improved genetic algorithm with initial population strategy and self-adaptive member grouping," *Computers & Structures*, vol. 86, pp. 1204-1218, 2008.

[18] O. Hasançebi, S. Çarbas, E. Dogan, F. Erdal, and M.P. Saka, "Performance evaluation of metaheuristic search techniques in the optimum design of real size pin jointed structures," *Computers & Structures*, vol. 87, pp. 284-302, 2009.

[19] A. Kaveh, and S. Talatahari, "Optimal design of Schwedler and ribbed domes via hybrid big bang–big crunch algorithm," *Journal of Constructional Steel Research*, vol. 66, no. 3, pp. 412-419, 2010.

[20] R. Su, X. Wang, L. Gui, and Z. Fan, "Multi-objective topology and sizing optimization of truss structures based on adaptive multi-island search strategy," *Structural and Multidisciplinary Optimization*, vol. 43, pp. 275-286, 2011.

[21] S. Gholizadeh, and A. Barzegar, "Shape optimization of structures for frequency constraints by sequential harmony search algorithm," *Engineering Optimization*, vol. 45, pp. 627-646, 2013.

[22] M. Babaei, and M.R. Sheidaii, "Automated optimal design of double-layer latticed domes, using particle swarm optimization," *Structural and Multidisciplinary Optimization*, vol. 50, pp. 221-235, 2014.

[23] O. Hasançebi, and S. Kazemzadeh Azad, “Adaptive dimensional search: A new metaheuristic algorithm for discrete truss sizing optimization,” *Computers & Structures*, vol. 154, pp. 1-16, 2015.

[24] A. Kaveh, and A. Boland-Gerami, “Optimal design of large-scale space steel frames using cascade enhanced colliding body optimization,” *Structural and Multidisciplinary Optimization*, vol. 55, pp. 237-256, 2017.

[25] P. Zakian, “Meta-heuristic design optimization of steel moment resisting frames subjected to natural frequency constraints,” *Advances in Engineering Software*, vol. 135, pp. 102686, 2019.

[26] M. Kociecki, and H. Adeli, “Shape optimization of free-form steel space-frame roof structures with complex geometries using evolutionary computing,” *Engineering Applications of Artificial Intelligence*, vol. 38, pp. 168-182, 2015.

[27] A.B. Templeman, “Heuristic methods in discrete structural optimization,” in *Discrete structural optimization (CISM courses and lectures no. 373)*, W. Gutkowski, Ed. New York: Springer-Verlag Wien, 1997, pp. 135-165.

[28] H.J.C. Barbosa, A.C.C. Lemonge, and C.C.H. Borges, “A genetic algorithm encoding for cardinality constraints and automatic variable linking in structural optimization,” *Engineering Structures*, vol. 30, pp. 3708-3723, 2008.

[29] M.I. Reitman, and W.B. Hall, “Optimal structural standardization,” *Engineering Optimization*, vol. 16, pp. 109-128, 1990.

[30] J.S. Angelo, H.S. Bernardino, and H.J.C. Barbosa, “Ant colony approaches for multiobjective structural optimization problems with a cardinality constraint,” *Advances in Engineering Software*, vol. 80, pp. 101-115, 2015.

[31] M. Galante, “Genetic algorithms as an approach to optimize real-world trusses,” *International Journal for Numerical Methods in Engineering*, vol. 39, pp. 361-382, 1996.

[32] L.A. Zadeh, “Optimality and non-scalar-valued performance criteria,” *IEEE Transactions on Automatic Control*, vol. 8, pp. 59-60, 1963.

[33] K. Shea, J.Cagan, and S.J. Fenves, “A shape annealing approach to optimal truss design with dynamic grouping of members,” *ASME Journal of Mechanical Design*, vol. 119, pp. 388-394, 1997.

[34] J.P.G. Carvalho, A.C.C. Lemonge, E.C.R. Carvalho, P.H. Hallak, and H.S. Bernardino, “Truss optimization with multiple frequency constraints and automatic member grouping,” *Structural and Multidisciplinary Optimization*, vol. 57, pp. 547-577, 2018.

[35] H.J.C. Barbosa, and A.C.C. Lemonge, "An adaptive penalty scheme in genetic algorithms for constrained optimization problems," in *Proc. GECCO'02*, New York: Morgan Kaufmann Publishers, 2002, pp. 287-294.

[36] J.P.G. Carvalho, A.C.C. Lemonge, P.H. Hallak, and D.E.C. Vargas, "Simultaneous sizing, shape, and layout optimization and automatic member grouping of dome structures," *Structures*, vol. 28, pp. 2188-2202, 2020.

[37] R. Storn, and K. Price, "Differential evolution a simple and efficient adaptive scheme for global optimization over continuous spaces," International Computer Science Institute, Berkeley, CA, Tech. Rep. 95-012, 1995.

[38] R.E. Bellman, *Dynamic Programming*, Princeton: Princeton University Press, 1957.

[39] S. Chen, J. Montgomery, and B.R. Antonio, "Measuring the curse of dimensionality and its effects on particle swarm optimization and differential evolution," *Applied Intelligence*, vol. 42, pp. 514-526, 2015.

[40] S. Kazemzadeh Azad, O. Hasançebi,and Saka M.P., "Guided stochastic search technique for discrete sizing optimization of steel trusses: a design-driven heuristic approach," *Computers & Structures*, vol. 134, 62-74, 2014.

[41] S.N. Patnaik, L. Berke, and R.H. Gallagher, "Integrated force method versus displacement method for finite element analysis," *Computers & Structures*, vol. 38, 377-407, 1991.

[42] S. Kazemzadeh Azad, and O.Hasançebi, "Discrete sizing optimization of steel trusses under multiple displacement constraints and load cases using guided stochastic search technique," *Structural and Multidisciplinary Optimization*, vol. 52, pp. 383-404, 2015.

[43] S. Kazemzadeh Azad, and S. Aminbakhsh, "High-dimensional optimization of large-scale steel truss structures using guided stochastic search," *Structures*, vol. 33, 1439-1456, 2021.

[44] Y.Y. Haimes, L.S. Lasdon, D.A. Wismer, "On a bicriterion formulation of the problems of integrated system identification and system optimization," *IEEE Transactions on Systems, Man, and Cybernetics,* vol. 1, pp. 296-297, 1971.

[45] American Institute of Steel Construction (AISC), "Manual of Steel Construction, Load & Resistance Factor Design," 2nd ed., Chicago, 1994.

[46] F.A. Charney, "The use of displacement participation factors in the optimization of drift controlled buildings," in *Proc. 2nd Conference on Tall Buildings in Seismic Regions, 55th Regional Conference*, Los Angeles, California, USA, 1991, pp. 91-98.

[47] H.S. Park, and C.L. Park, “Drift control of high-rise buildings with unit load method,” *The Structural Design of Tall Buildings*, vol. 6, 23-35, 1997.

[48] F.A. Charney, “Economy of steel framed buildings through identification of structural behavior,” in *Proc. National Steel Construction Conference*, Orlando, FL, 1993, pp. 1-33.

[49] “Formian-2 software” Available: www.formexia.com/software.aspx [Accessed: June 17, 2021]